



UPPSALA
UNIVERSITET

*Digital Comprehensive Summaries of Uppsala Dissertations
from the Faculty of Science and Technology 609*

Thin Film Electroacoustic Devices for Biosensor Applications

GUNILLA WINGQVIST



ACTA
UNIVERSITATIS
UPSALIENSIS
UPPSALA
2009

ISSN 1651-6214
ISBN 978-91-554-7432-4
urn:nbn:se:uu:diva-89424

Dissertation presented at Uppsala University to be publicly examined in Å2005, Ångströmlaboratoriet, Lägerhyddsvägen 1, Uppsala, Friday, March 27, 2009 at 10:15 for the degree of Doctor of Philosophy. The examination will be conducted in English.

Abstract

Wingqvist, G. 2009. Thin Film Electroacoustic Devices for Biosensor Applications. Acta Universitatis Upsaliensis. *Digital Comprehensive Summaries of Uppsala Dissertations from the Faculty of Science and Technology* 609. 96 pp. Uppsala. ISBN 978-91-554-7432-4.

Biosensors are today important devices within various application areas.

In this thesis a new type of *label-free biosensor* device is studied, which is fabricated using the same processes used for the fabrication of integrated circuits. This enables tighter integration and further sensors/biosensor miniaturization. The device is a so-called *Thin Film Bulk Acoustic Resonator (FBAR)*. Within this thesis a low temperature reactive sputtering process for growing AlN thin films with a c-axis inclination of 20-30° has been developed. This enables *shear mode FBAR* fabrication suitable for in-liquid operation, essential for biosensor applications. Shear mode FBARs were fabricated operating at frequencies above 1GHz exhibiting Q values of 100-200 in water and electromechanical coupling factors k_t^2 of about 1.8%. This made it possible to move the thickness excited shear mode sensing of biological layers into a new sensing regime using substantially higher operation frequencies than the conventionally used quartz crystal microbalance (QCM) operating at 5-20MHz. Measured noise levels of shear mode FBARs in contact with water showed the resolution to be in the range 0.3ng/cm² to 7.5ng/cm². This demonstrated the FBAR resolution without any averaging or additional stabilization measures already to be in the same range as the conventional QCM (5ng/cm²), suggesting that FBARs may be a competitive and low cost alternative to QCM. The linear thickness limit for sensing of biomolecular layers was concluded to be larger than the thickness of the majority of the molecular systems envisaged for FBAR biosensor applications. A temperature compensated shear mode FBAR composite structure was demonstrated with retained coupling factor and Q-value by utilizing the second mode of operation. Understanding has been gained on the sensor operation as well as on how the design parameters influence its performance. Specifically, sensitivity amplification utilizing low acoustic impedance layers in the FBAR structure has been demonstrated and explained. Further, temperature compensated Lamb mode (FPAR) devices were also studied and demonstrated with optimized electromechanical couplings.

Keywords: aluminium nitride; FBAR; shear mode resonator; lamb wave device; liquid sensor; biosensor; reactive sputtering; temperature compensation

Gunilla Wingqvist, Department of Engineering Sciences, Solid State Electronics, Box 534, Uppsala University, SE-75121 Uppsala, Sweden

© Gunilla Wingqvist 2009

ISSN 1651-6214

ISBN 978-91-554-7432-4

urn:nbn:se:uu:diva-89424 (<http://urn.kb.se/resolve?urn=urn:nbn:se:uu:diva-89424>)

Included Papers

- I. J. Bjurström, G. Wingqvist, and I. Katardjiev, "**Synthesis of textured thin piezoelectric AlN films with a nonzero C-axis mean tilt for the fabrication of shear mode resonators**" IEEE Transactions on Ultrasonics, Ferroelectrics and Frequency Control, vol 53, issue 11, p 2095 – 2100, 2006.
- II. J. Bjurström, G. Wingqvist, V. Yantchev and I. Katardjiev, "**Temperature Compensation of Liquid FBAR Sensors**", Journal of Micromechanics and Microengineering, v 17, issue 3, p 651-8, 2007.
- III. G. Wingqvist, J. Bjurström, L. Liljeholm, V. Yantchev, and I. Katardjiev, "**Shear mode AlN thin film electro-acoustic resonant sensor operation in viscous media**", Sensors and Actuators, B: Chemical, vol. 123, pp. 466-473, 2007.
- IV. G. Wingqvist, J. Bjurström, A-C. Hellgren and I. Katardjiev, "**Immunosensor utilizing Shear mode thin film bulk acoustic sensor**", Sensors and Actuators B: Chemical, Volume 127, Issue 1, p 248-252, 2007.
- V. G. Wingqvist, V. Yantchev, I. Katardjiev, "**Mass sensitivity of multilayer thin film resonant BAW sensors**", Sensors and Actuators A: Physical, v 148, issue 1, p 88-95, 2008,
- VI. G. Wingqvist, H. Andersson, C. Lennartsson, V. Yantchev, A. Lloyd Spetz "**On the applicability of high frequency shear mode acoustic biosensing in view of thickness limitations**", submitted to Biosensors and Bioelectronics.
- VII. G. Wingqvist, A. Arapan, V. Yantchev, I. Katardjiev "**Micro-machined thermally compensated thin film Lamb wave resonator for frequency control and sensing applications**" Accepted for publication in Journal of Micromechanics and Microengineering

Description of my contribution

- I. Part of experimental verification of the process and shear mode operation. Part of fabrication.
- II. Part of experimental work and fabrication.
- III. Planning of paper focus and content with input from co-worker, major part of mathematical model implementation and calculations, writing with extensive input from co-worker. Part of experimental work and part of fabrication.
- IV. All FBAR experimental work and calculations writing with input from coworkers.
- V. Planning of paper focus and content with input from co-worker. All mathematical model implementation and calculations. Large part of experimental testing and fabrication. Writing with extensive input from co-worker.
- VI. Planning of paper subject and content with essential input from coworkers in terms of experimental execution. Part of FBAR experimental testing. All calculations. Writing with input from co-workers.
- VII. Part of fabrication. Part of calculations. Part of experimental testing. Part of writing

Related Publications

- i. J. Bjurström, G. Wingqvist, and I. Katardjiev, "Synthesis of textured thin piezoelectric AlN films with a nonzero c-axis mean tilt," IEEE Ultrasonics Symposium, Rotterdam, The Netherlands, 2005.
- ii. G. Wingqvist, J. Bjurström, L. Liljeholm, I. Katardjiev, and A. L. Spetz, "Shear Mode AlN Thin Film Electroacoustic Resonator for Biosensor Applications," IEEE Sensor, Irvine, Ca, USA, 2005.
- iii. G. Wingqvist, J. Bjurström, A-C. Hellgren and I. Katardjiev, "Immunosensor utilizing Shear mode thin film bulk acoustic sensor", Eurosensors XX, Gothenburg, Sweden, 2006.
- iv. J. Bjurström, G. Wingqvist, V. Yantchev, and I. Katardjiev, "Design and Fabrication of Temperature Compensated Liquid FBAR Sensors" IEEE Ultrasonic Symposium, Vancouver, Canada, 2006.
- v. G. Wingqvist, V. Yantchev, J. Bjurström, and I. Katardjiev, "Mass Sensitivity of Thin Film Resonator Devices ", IEEE Freq Control Symp, Geneva, Switzerland, 2007.
- vi. G. Wingqvist, L. Arapan, V. Yantchev, and I. Katardjiev, "Temperature Compensation of Thin AlN Film Resonators utilizing the Lowest order Symmetric Lamb mode," Ultrasonic Symposia, Beijing, China, 2008.
- vii. A. Lloyd Spetz, S. Nakagomi, H. Wingbrant, M. Andersson, A. Salomonsson, S. Roy, G. Wingqvist, I. Katardjiev, M. Eickhoff, K. Uvdal, R. Yakimova, "New materials for chemical and biosensors", Materials and Manufacturing Processes, v 21, n 3-4, p 253-6, 2006.
- viii. I. Katardjiev, J. Bjurström, and G. Wingqvist, "Production of polycrystalline films for shear mode piezoelectric thin film resonators", International patent application PCT/SE2006/050041, 2006 ed Sweden, 2006.

Contents

Preface	11
Chapter 1 Introduction	13
1.1 Sensor fundamentals	16
1.1.1 Sensitivity	16
1.1.2 Sensor Categories	17
1.2 Biosensor	18
1.2.1 Transducer principles.....	18
1.2.2 Biological recognition element and the necessity for liquid environment	19
1.3 Electroacoustic technology.....	20
1.3.1 Piezoelectric material.....	20
1.3.2 Electroacoustic resonator sensor operation.....	21
1.3.3 Quartz Crystal Microbalance (QCM)	24
1.3.4 Thin film electroacoustic technology	26
1.3.5 State of the art of the shear mode FBAR technology	29
Chapter 2 Tilted Film Deposition process [Paper I]	31
2.1 AlN and the electro-acoustic excitation dependence on the crystalline orientation.....	31
2.2 Description of the two-step deposition process for c-axis inclined AlN thin film	33
2.3 Discussion on the tilted film process.....	34
Chapter 3 Shear mode FBAR biosensor – design and fabrication [Paper I, II].....	37
3.1 Membrane FBAR versus Solidly Mounted FBAR.....	38
3.2 Microfluidic channel	39
3.3 Sensor surface	40
3.4 Temperature compensation of shear mode FBAR	41

Chapter 4 Shear mode FBAR sensor – performance and characteristics [Paper III - VI]	45
4.1 Noise and resolution	45
4.1.1 Electrical Characterization	47
4.2 In-liquid performance	49
4.2.1 Verification of the Shear mode	49
4.2.2 Influence of polarization angle and electromechanical coupling on the FBAR in-liquid dissipation	49
4.2.3 The Shear mode FBAR utilized as s Biosensor	51
4.3 Mass sensitivity	51
4.3.1 Theoretical background	53
4.3.2 Mass sensitivity Analysis of Composite resonator structures and sensitivity amplification	53
4.3.3 Summary of mass sensitivity results [Paper V]	54
4.4 Sensing of biomolecular layers and thickness limitations due to film resonance	55
4.4.1 Biomolecular modeling	56
4.4.2 Amplitude distribution and effective thickness	57
4.4.3 Film resonance	58
Chapter 5 Lamb mode waves and devices [Paper VII]	61
5.1 Lamb modes	61
5.2 Lamb modes in FBARs	62
5.2.1 Lamb modes in c-axis inclined AlN FBAR	63
5.3 Lamb mode devices - Thin film plate acoustic resonators (FPAR) ..	64
5.4 Temperature stabilized FPAR	66
Chapter 6 Concluding remarks and Further Discussion	69
6.1 Findings	70
Chapter 7 Sammanfattning på svenska	73
References	77
Appendix A Sputtering	85
Appendix B AlN	89
Appendix C Fabrication of a typical FBAR sensor	91
Appendix D Simulation models and implementation of the Mason model ..	93

Abbreviations

AFM	Atomic Force Microscopy
BAW	Bulk Acoustic Wave
BSA	Bovine Serum Albumin
EA	Electroacoustic
FBAR	Thin Film Bulk Acoustic Resonator
FPAR	Thin Film Plate Acoustic Resonator
IDT	Inter-Digital Transducer
LFE	Lateral Field Excited
POC	Point of Care
QCM	Quartz Crystal Microbalance
QCM-D	Quartz Crystal Microbalance with Dissipation monitoring
SAW	Surface Acoustic Wave
SEM	Scanning Electron Microscopy
SMR	Solidly Mounted Resonator
TE	Thickness Excited
XPS	X-Ray Photoelectron Spectroscopy
XRD	X-Ray Diffraction

Preface

The main focus of this thesis has been to study the applicability of a new type of sensor transducer device (the shear mode thin film bulk acoustic resonator – shear mode FBAR) for biosensor applications in terms of sensitivity, noise performance, temperature stability, in-liquid performance (essential for biosensing) and detection distance in view of biomolecular layer thicknesses. Understanding has been gained on the sensor operation as well as on how the design parameters influence the performance.

This thesis has been conducted at Uppsala University. Part of this PhD thesis project has belonged to a Vinnova funded project together with Biosensor Application AB and Linköping University. Another part of this PhD thesis project has belonged to the EU-funded project entitled Integrated Biosensor System for Labelfree In-vitro DNA and Protein Diagnostics in Healthcare Applications (Biognosis) and coordinated by Siemens AG. The project consisted of several partners¹ where Uppsala University's role was in the development of the FBAR biosensor array.

The author has actively performed every design, process and characterization step needed for fabrication of the FBAR sensor. In addition the author has conducted and developed the electrical characterization, as well as implemented and utilized simulation models in Matlab and Mathematica. Some simulations using ADS has also been performed.

All fabrication steps from the mask design to the deposition of piezoelectric active layer, metallization and etching have been performed in the clean room facilities at Uppsala University. At these facilities material characterization utilizing XPS, SEM, EDS and AFM has also been performed. The electrical characterization setup was developed and used at the lab of the Solid State Electronics Department, Uppsala University. The

¹ Siemens Aktiengesellschaft (D) – Industry, Biosensor Application Sweden AB (S) – Industry, VTT Technical Research Centre of Finland (FIN) – Governmental, Cranfield University (GB) – University, Medizinische Universität Innsbruck (A) – University, Uppsala Universitet (S) – University, Perlos OYJ (FIN) – Industry.

XRD equipment at the Material Chemistry Department, Uppsala University, was frequently utilized for film characterization.

The thesis has the following outline:

First, there is an introduction to the field of sensors in general and biosensors specifically, followed by introduction to the electro-acoustic technology and the thin film technology.

Then there is a presentation and summary of the research conducted within this thesis; divided into 4 different chapters. The main results are then summarized and discussed. Some specific details and longer descriptions can be found in the appendixes.

In the final part the included papers are found.

I would like to thank all the authors of the included papers for their contributions.

I would also like to take the opportunity to especially thank the persons to whom I am extra grateful for their help and support in finalizing this work.

Dr Ventsislav Yantchev: acting as my actual supervisor/teacher, never truly content, but always willing to discuss.

Henrik Andersson and *Dr. Ann-Charlotte Hellgren*: for patiently answering my questions about biochemistry and biosensor applications.

Dr Johan Bjurström: for introducing me to the work in the clean room and the tilted AlN film process and for being patiently supportive during my first years in Uppsala.

The *MSL personnel* for all the help on the battlefield we like to call “down in the cleanroom”.

Professor Anita Lloyd Spetz: for all your encouragement and support

Professor Ilia Katardjiev, *Professor Jörgen Olsson* and *Dr. Joakim Andersson* for careful reading of this thesis

And my friend *Dr Lars Vestling* for your skills in everything computer related and for patiently listening to my continuous monologues about work related issues. Och för att du bara låter mig vara som jag är.

Uppsala, 2009

Gunilla Wingqvist

Chapter 1

Introduction

Human beings have always tried to control their environment in order to protect themselves. Fast and correct information is the key to enable effective actions, reactions and precautions. The main tools for retrieving information have been our senses. The five senses are traditionally sight, hearing, touch, smell and taste.² Our senses are however in many cases not enough. Human beings have therefore continuously improved and developed methods and equipments to act as extensions of their own senses. This has been done for several reasons:

Firstly, we want to receive absolute *objective values* of various properties in order to simplify communications with each other. For example, we want to have a measure of the weight of a piece of gold in order to agree fairly on its value.

Secondly, we want to receive information *without exposing our self*. For example, we want to know if the oven is warm enough without placing our hand in it.

Thirdly, we want to *improve our senses*. We want to hear sounds and see lights, which are outside our sensing range; we want to detect very large things on large distances (like the planets and the solar systems); we want to detect very small things (molecules or atoms).

To enable gathering of more information with improved accuracy about our environment has been one of the key prerequisites for technical and medical developments in general. The increased amount of gathered information can however only be beneficial to a certain extent if it is not stored and processed properly. The developments in the electronic industry the last decades have made it possible to store and process tremendous amount of information, which has opened up the usefulness for sensing tools that can be communicated with

² In modern science, the senses could actually be categorized into at least twice as many categories.

by an electrical signal. Such sensing tools are generally called *sensors*. In the history of human beings, a sensor is by the above definition an extremely new type of device and its full potential can thereby not yet be foreseen. There are however some very promising areas of applications, such as public defense, health care, agriculture and food quality monitoring.

As mentioned in the beginning, one of the main reasons for our desire to understand and control our environment is to protect our self. We would like to protect our self from harmful chemicals (solid, liquid or gas) and biological species (e.g. viruses or bacteria). We want to know at an early stage when we are sick. The developments in the chemical and biomedical research have improved the understanding of our bodies on the molecular level opening up the possibility to receive early diagnosis from blood, urine or saliva samples without dangerous surgery or hurtful testing.

The developments in the molecular chemistry together with the computerized storing, processing and sharing of data have opened up the possibilities for point of care (POC) applications. POC refers to the ability to perform diagnostic procedures in a precise and rapid manner at the site where it is needed (i.e. in the doctors office, on the battle-field or on-site in greenhouses or the field.) Furthermore, the procedure should be able to be performed by non-specialist personnel with basic training. The data communication technology enables rapid enquires with a non-localized specialist if necessary.

Biosensors are one of the most important types of sensors for applications where *precise and selective* detection of target molecules is required. The detection is done by customized bio-molecules, for example antibodies. In addition, biosensors are an important tool for analytical research studies of biomolecular interactions with other various molecules (drug or diagnostics development) or with solid surfaces (in view of for instance verifications of body implants).

Continuing miniaturization is the key driver for the POC sensor development for usage in homes, at the doctor's office or at hospitals as well as in the area of defense and public safety.

Further barriers to the introduction and wide spread use of sensors are in many cases the cost and compatibility to the associated electronics. Sensors require, therefore, to be integrated with electronics either in a monolithic or at least hybrid form. The electronics is necessary for driving and detecting the sensors as well as processing the gathered information. In many of the medical and environmental sensor applications, there will also be a need for the sensor system to autonomously initiate an action according to the processed sensor information. This action is also most likely to be controlled and driven by electronics.

It would therefore be beneficial, in view of further sensors/biosensor miniaturization, to fabricate the transducers utilizing the same technology as used for the electronics in order to enable tighter integration. The integrated circuit (IC) technology has proven to be able to simultaneously mass fabricate thousands of electronic devices placed on a single wafer.

The tremendous development of the electronics industry in the last decades has been enabled in part by the *thin film technology* and the elaborate processes of etching and deposition of such thin material layers onto a substrate (usually silicon). To mass fabricate sensor transducers directly onto the same, or the same type of substrates used for the driving and supporting electronics, using compatible technologies, would undoubtedly open up the potential for new sensors and sensor applications. Therefore, the thin film technology in general has raised an increasing interest for various types of applications.

Specifically the thin film *electro-acoustic* technology employing piezoelectric thin film materials has in the last two decades made tremendous advances, primarily driven by filter applications for the telecom industry, utilizing *thin film bulk acoustic resonators* (FBAR). Such FBAR filters have been in commercial products since 2001, particularly in mobile phones.

The recent development of the so-called *shear mode* FBAR, presented inhere, has paved the way for a second major application of the thin film electro-acoustic technology, namely the fabrication of highly sensitive, miniature biosensors and, therefore, opened up the possibility for truly integrated and miniaturized biosensor and biosensor array systems.

Further, research in thin film electro-acoustics is still in its initial phase and other types of devices e.g. thin film plate acoustic resonators (FPAR), are constantly emerging, which widens up the potential of this technology even further.

The primary focus of this project has been to investigate and develop the shear mode FBAR technology. The main efforts have been devoted to the description and understanding of the operation of the shear mode FBAR transducer platform, in view of biosensor applications. This has been done mainly in view of verification of the applicability of the new technology with regard to sensitivity, resolution and detection distance.

A secondary focus of this project has been the area of acoustic sensing at microwave frequencies enabled by the thin film technology. Acoustic sensing explores the acoustic properties of the bio-molecular layers; i.e. density, viscosity and stiffness. Scanning of such properties at various frequencies could allow for further knowledge of bio-molecular systems.

Finally, certain developments on FPAR devices have been performed in addition to initial investigations of the technology in view of possible general sensor applications.

1.1 Sensor fundamentals

***Sensor** is a device that detects or measures a physical property and records, indicates, or otherwise responds to it.*

- The Oxford Pocket Dictionary of Current English

A sensor is converting a physical quantity, or a change in a physical property, into a detectable, often electrical, signal. The development within the microelectronics has given sensors and sensor systems producing electrical signals enormous capabilities to process and store received data within the sensor unit directly or in external computer units.

1.1.1 Sensitivity

Sensitivity is one of the most fundamental properties of a sensor. Therefore, it is striking to note the confusion present concerning the use of the term ‘sensitivity’. In the sensor science text books in general, as well as within this thesis, the definition used is:

Sensitivity (S): The sensor output per unit of measurand,

where the sensor output often is a change in sensor signal and the measurand is the variable to be measured. However, in practical use the term ‘sensitivity’ is often used in the same manner as what in the sensor science is referred to as ‘resolution’; that is:

Resolution (R): The smallest detectible amount of measurand.

In the majority of sensor applications, the ‘resolution’ is the main concern and the limiting factors of the resolution are the noise and the sensitivity. The noise is fluctuations in the output signal not caused by the measurand. Sensor noise is caused by internal thermal and electrical vibrations of the transducer, as well as of variation of external variables such as temperature, pressure or electric fields. In biosensors in addition to that, the variation in viscosity and electrical properties of the bulk fluid as well as unspecific binding cause undesirable shifts in the output signal. These unwanted continuous variations in the signal will create a noise floor, which limits the smallest detectable signal (δ). The resolution (R) is consequently defined by the ratio between the smallest detectable signal (δ) and the sensitivity (S) as:

$$R = \frac{\delta}{S} \cdot$$

Other important sensor properties are the linearity, dynamic range; that is, the range of measurand amount within which the sensitivity accuracy can be guaranteed.

1.1.2 Sensor Categories

Sensors are categorized in many different ways; by the type of measurand they measure, the type of transduction principle they employ or by the fabrication technology by which they are manufactured. When different types of recognition on molecular level are concerned, the sensors could also be categorized by the type of recognition reaction used; primarily chemical or biological.

This variety of sensor categorization could be rather confusing, leading to misleading or at least non-accurate conclusions of the present market shares and statistics on the type of sensors being of main research interest. In the last decade, the most evident example is the term MEMS (*Micro Electromechanical System*) sensor, which refers to the micro-fabrication technology employed in combination with the applied electro-mechanical transduction principle. It is sometimes compared to sensor categories based on sensor application aspects consequently leading to non-adequate analysis of the result.

Further, the term MEMS, a frequently used term in the last decades, could refer to various types of devices depending on the community and context. In a general sensor context MEMS sensor is defined as above. However, in the *ultrasonic* community the term almost exclusively refers to silicon (or polymer) based freestanding mechanical structures, which are activated electro-statically or by use of piezoelectric materials. Therefore, the thin film bulk acoustic resonator (FBAR), where the mechanical vibrations are primarily confined to a piezoelectric material, not in silicon, is *never* referred to as MEMS resonator. The thin film plate mode acoustic resonator (FPAR), could, however sometimes be referred to as a MEMS device, even though the vibrations are contained in the piezoelectric thin film, since the acoustic vibration is more similar to the ones seen in the silicon structures.

Both the FBAR and FPAR are categorized under *electroacoustic devices*, in analogy with the single crystalline based devices such as *Quartz Crystal Microbalance* (QCM) and *Surface Acoustic Wave* (SAW) devices. All devices mentioned above are used for sensor applications; physical, chemical and biological.

1.2 Biosensor

In the context of this thesis, the term *biosensor* is applied for sensors using biomolecules as selective recognition elements. These biological recognition elements selectively react with the analyte and the biochemical reaction is then recorded by a transducer, which is sending a signal to the read-out unit. In fig. 1 the principle of a general biosensor is illustrated.

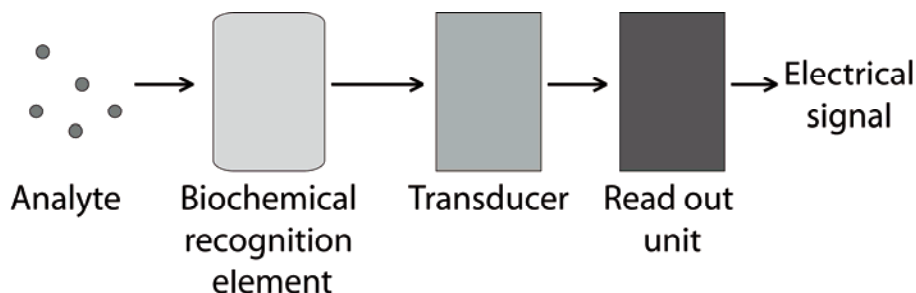


Figure 1. *Schematic definition of a general biosensor*

Biosensors are used for detecting target molecules, such as narcotics and explosives (Biosensor Applications AB, Sweden) or for analytical studies of bimolecular interaction with other molecules or with solid surfaces (Biacore, Sweden; Attana, Sweden or Q-Sense, Sweden).

The recognition procedure can be divided into *label-dependent* (recognition molecules are conjugated to enzymes or fluorescent markers) or *label-free* detection (e.g. antibodies need not be labeled with fluorophores, radioisotopes, colloidal gold particles or enzymes for detection of binding events or signal enhancement). So far the label-dependent sensors have been dominating, but the more easy-to-use label-free detection principle has received growing attention in the last decades.[1, 2] The main transducer principles for the label-free sensors are the *surface plasmon resonance* (SPR) and the electroacoustic devices (i.e. QCM).

1.2.1 Transducer principles

The electro-acoustic devices (QCM, SAW, FBAR, FPAR and so on) and MEMS resonators are usually called gravimetric sensors, due to their supposedly proportional response towards mass loading onto the surface; the response is primarily a variation in the mechanical resonance frequency. The term gravimetric is somewhat misleading especially when biosensor applications are concerned. Herein the term *acoustic sensors* will be employed to indicate that the sensors sense changes in acoustic properties (density, elasticity and viscosity) due to for instance biochemical reactions. This term fits also very well with the commonly used terminology for

categorizing other types of biosensor transduction principles; thermal sensors – sense temperature changes due to biochemical reactions, optical sensors – sense changes in optical properties due to biochemical reactions, electrochemical sensors – sense electrical potential or current change due to biochemical reactions.

1.2.2 Biological recognition element and the necessity for liquid environment

Biomolecules used as recognition elements in biosensors could be based on either proteins, such as antibodies, enzymes and receptors or nucleic acids such as aptamers. Enzymatic biosensors use enzymes, which usually act as catalysts for chemical reduction-oxidation reactions generating/consuming heat and electrical charges and are, therefore, most suitable for thermal or electro-chemical transducer principles. For the electro-acoustic resonator transducer principle the reaction must result in a binding to or release of molecules from the surface, where the most common approach is the use of antibodies (immunosensing), or various engineered derivatives such as antibody fragments (Fab) or single chain variable fragments (scFv). In fig. 2 the electroacoustic biosensor principle is illustrated.

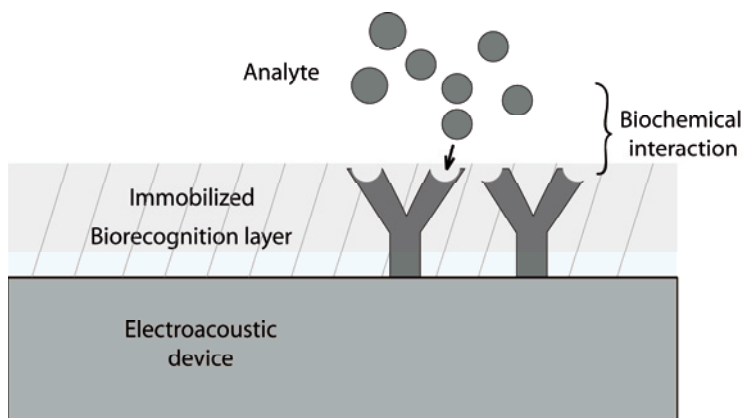


Figure 2. *Schematic drawing of a electroacoustic biosensor*

The antibodies and their derivatives are proteins containing amino acids linked together by peptide bonds, which are strong covalent bonds restricting the rotation possibilities at these points. The protein will have a 3-dimensional structure depending on the interactions between the amino acids themselves and with the surrounding media. The interactions include Coulomb, dipole-dipole, van der Waals, or hydrophobic interactions, and often all of these must be present in order to preserve the three dimensional structure of the protein and consequently the functionality of the protein. Therefore, all analysis involving proteins or other biomolecules as selective

recognition element must take place in an aqueous and saline environment with well-controlled pH and salt concentration, i.e an environment in which proteins are normally found.

If the protein is removed from its native environment, the three dimensional structure of the protein will be disrupted and the functionality will be lost. It is consequently essential for the applicability of the FBAR biosensor utilizing protein-based biochemistry to operate with high performance in a liquid environment.

1.3 Electroacoustic technology

Electroacoustics deals with the transformation of acoustic energy into electric energy or vice versa. Most often this transformation is conducted within a *piezoelectric* material.

Electroacoustic wave devices based on piezoelectric materials have been in commercial use for over 60 years. The applications for the electroacoustic technology range from frequency control, sonar and ultra sound investigations, filter applications, sensors, etc. So far, the most common configurations have been *bulk acoustic wave* (BAW) devices and *surface acoustic wave* (SAW) devices. These devices are used in almost all time and frequency control applications. The telecom industry alone consumes billions of filters annually.

1.3.1 Piezoelectric material

Piezoelectric materials are dielectric crystals belonging to a non-centre symmetric point group, which could mean two things. First, the gravity centre of the positive and the negative charges do not coincide causing a total dipole moment in the crystal (a polar crystal). Second: the gravity centers of positive and negative charges do coincide (non-polar crystal) but not in the centre of the unit cell.

An applied stress to the crystal will then result in a change in the dielectric polarization, inducing a change in the electric field in the crystal. Similarly, an electric field applied to the crystal will cause the crystal to become strained. The strain will induce an acoustic wave. The anisotropy of the crystal will cause the mode, velocity and direction of the excited wave to strongly depend on the crystal direction. Due to the piezoelectricity the acoustic wave will in its turn have an electric field coupled to it, depending on the mode and direction.

When it comes to polycrystalline materials it is important to consider the symmetry of the complete multigrain system. The randomness of the grains could cause the piezoelectricity to be canceled in certain directions due to the introduction of symmetry.

1.3.2 Electroacoustic resonator sensor operation

In here the main focus will be on the so-called thickness excited bulk wave resonator (BAW), that is, it represents a parallel plate acoustic resonator generally made of a piezoelectric material in which acoustic waves are generated by applying an electric field perpendicular to the plate and are subsequently reflected by the plate edges. Schematic illustration of excited and reflected waves inside a resonance cavity can be seen in fig. 3.

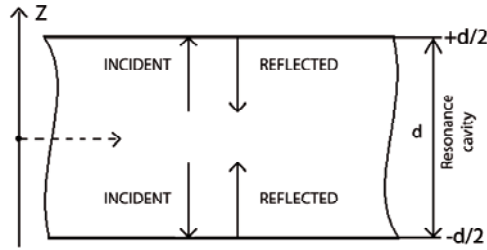


Figure 3. *Schematic illustration of excited and reflected waves inside a resonance cavity*

The electric field is often applied in a sinusoidal alternating manner and at the *resonance frequency* the excited and reflected waves interfere in a constructive manner inside the cavity; that is, *mechanical resonance* occurs.

The resonance frequency depends on the resonance cavity (configuration, material properties and thicknesses) and the surrounding media in contact with the resonator. Further, the properties of all materials involved and consequently the resonance frequency is directly affected by temperature and stresses. Approximately the resonance occurs for frequencies given by the condition for wave synchronism $f = V_{\text{WAVE}}/\lambda$, where V_{WAVE} is the acoustic wave velocity and λ is the acoustic wavelength. Typically, BAW resonators operate at frequencies, corresponding to standing wave formation, defined at wavelengths $\lambda = 2d/n$, where $n = 1, 2, 3, \dots, 2k+1, \dots, \infty$, represents the harmonic of operation and d is the thickness of the resonator. Electrically, only odd harmonics can be excited. In composite resonator structures, however, even harmonics of operation could be excited too. The mode excitations in single as well as composite thickness excited resonator structures are shown in fig. 4.

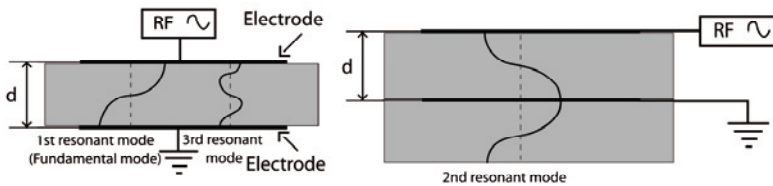


Figure 4. *Illustrations of the mode excitations in single as well as composite thickness excited resonator structures*

The electrical response (fig. 5) is identical to an *electric resonance response* combining *series resonance* and *parallel resonance* at closely placed frequencies. For FBARs the series resonance frequency corresponds to the mechanical resonance and the separation to the parallel resonance frequency is then related by the *electromechanical coupling coefficient*, defined from the ratio of the mechanical energy to the electrical energy³. For lateral excitation the situation is the reversed.

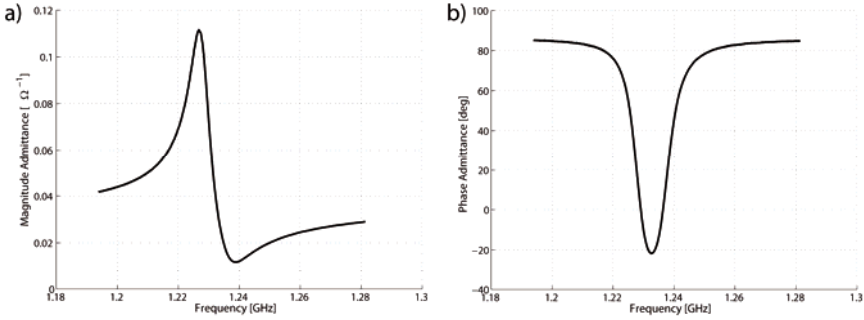


Figure 5. *Measured admittance response of 2 μm shear mode AlN FBAR operating at 1.52GHz in contact with water on one side, showing the series resonance at about maximum admittance (zero phase, negative phase slope) and parallel at about minimum admittance (zero phase, positive phase slope).*

Modeling

The electrical response can simply be described by the lumped equivalent circuit model of Butter-Van Dyke (BVD) shown below in fig. 6. Most generally the model describes the resonator as a *clamped capacitor* (describing the resonator outside resonance) in parallel with a *motional arm* (describing the resonator near mechanical resonance). In an ideal resonator (the motional resistance $R_m=0$) the motional arm will be short-circuited at resonance and hence all the energy will pass through the motional arm.

³ The electromechanical coupling describes the efficiency of the electromechanical excitation. For the FBAR the electromechanical coupling can be approximated by $(\pi^2/4)(f_p-f_s)/f_p$, where f_s and f_p are the series and parallel resonance frequency respectively.

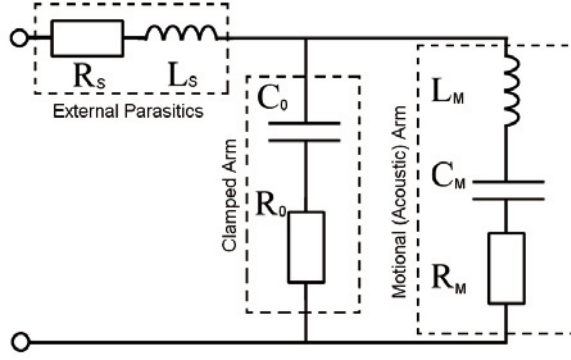


Figure 6. *Butterworth-Van Dyke (BVD) equivalent model of a piezoelectric resonator*

The electrical and mechanical response can further be described and simulated by utilizing the general transmission line model, where the Mason model [3] is one of the most widely used within the electroacoustic community. The model and its implementation is presented more thoroughly in Appendix D. Another model also used within this thesis is derived by Nowotny and Benes[4]. The model gives the opportunity to easily calculate the response in various crystal directions using matrix formalism. Both the Mason and Nowotny-Benes models are one-dimensional meaning that the wave is assumed to be a planar wave propagating orthogonally to the boundaries and the layers in the structure to be homogeneous. They will however also take into account the area; i.e. the clamped capacitor.

Wave propagation

Acoustic waves in isotropic solids have either longitudinal or transverse polarization, generating compressional or shear deformation. In anisotropic solids there can exist quasi modes with both longitudinal and transverse polarization components. Fluids such as air or water can support only longitudinal waves since their shear modulus is zero. Therefore, for in-liquid operating thickness excited bulk acoustic wave as well as for surface acoustic wave devices, shear wave motion is required, confining in this way the acoustic energy to the resonator cavity or equivalently avoiding acoustic leakage into the surrounding medium. Fundamental mode of longitudinal and shear mode motion in a piezoelectric slab through thickness excited actuation is illustrated in fig. 7.

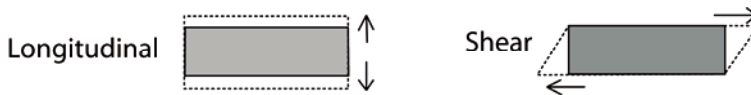


Figure 7. *Fundamental longitudinal mode and shear mode motion in a piezoelectric slab through thickness excited actuation*

Due to the frictional forces within viscous media there will be however some highly damped shear motion translated into the liquid (fig. 8), causing the resonator to be affected by acoustic property variations within a small detection distance from the sensor surface. This is the base for biosensor operation with shear mode electroacoustic devices.

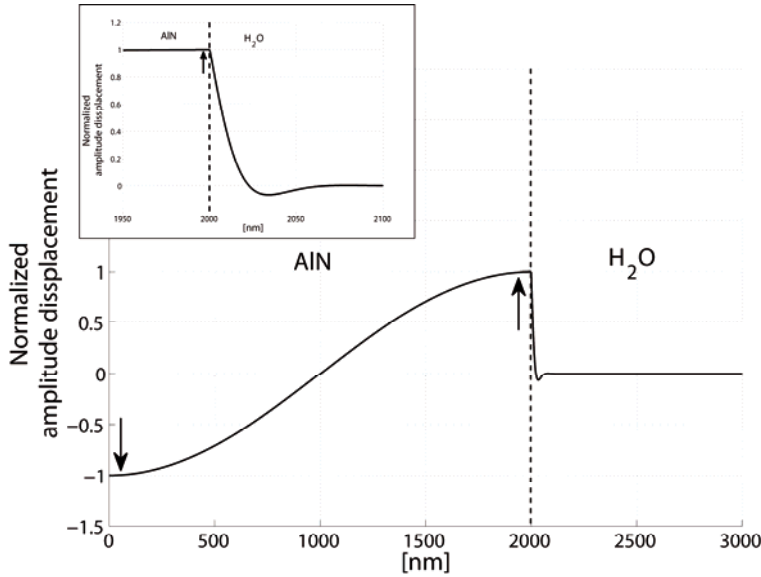


Figure 8. *Displacement distribution calculated for a 2 μ m AlN shear mode resonator operating at 1.52GHz in contact with water, normalized to the displacement at AlN surface. The distribution is calculated for a moment near maximum strain in the AlN.*

1.3.3 Quartz Crystal Microbalance (QCM)

The quartz crystal microbalance (QCM) is the most commonly used electroacoustic sensor and the principle is the same as for the shear mode FBAR. It consists of a circular single crystal quartz disc with centre symmetrically placed electrodes on each side creating an applied electric field across the thickness of the disc. The quartz disc is in the case of QCM cut along its so-called AT-direction causing the excited acoustic wave to be shear-polarized and temperature compensated around room temperature, making it a stable choice for in-liquid as well as in-air sensor applications. The fundamental frequency of QCM is typically 5-20MHz and the disc is typically just below 1cm in diameter, with an active area with about half that diameter. Higher frequency and smaller size QCMs are also available. However, special expensive high quality polishing and microstructure etching is then required.

The quartz crystal technology is a lumped device, which cannot be fabricated onto a silicon substrate along with the electronics, but needs to be connected to the circuitry separately by probing or bonding.

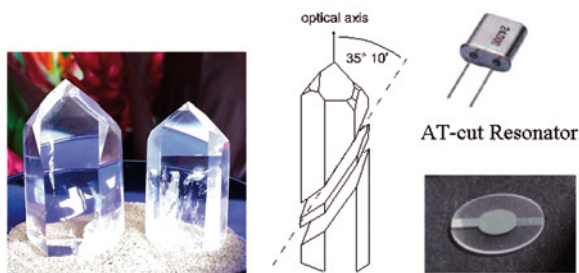


Figure 9. *Quartz crystal microbalance (QCM) consists of AT-cut slab of a quartz crystal.*

Historical background of QCM

The signal transduction mechanism of the QCM technique relies upon the piezoelectric effect first reportedly discovered in 1880 by the Curie brothers [5]. A change in inertia of a vibrating piece of solid material was then shown by Lord Rayleigh to alter its resonant frequency [6]. Important subsequent developments were good crystal stability through the use of electric resonators[7] and room-temperature stable AT-cut crystals [8]. In 1959, the QCM was first used in a sensing mode when Sauerbray reported a linear relationship between the frequency decrease of an oscillating quartz crystal and the bound elastic mass [5, 6]. Early chemical applications of QCM included the measurement of mass binding from gas-phase species to the quartz surface directly or onto the quartz surface covered with other materials [9-12]. These also represented some of the earliest chemical sensors for moisture and volatile organic compounds [13]. In the 1980s, new oscillator technology enabled to measure changes in QCM frequency that could be related to changes in viscosity and density in highly damping liquid media [14-16]. The frequency shift due to changes in viscosity and density in liquids derived was in essence similar to earlier findings of the viscosity and density dependence in gases[17]. The operation in liquid media enabled utilizing the QCM for biosensor applications. In the mid 90's a new QCM measurement technique (QCM-D) emerged which in addition to measuring resonance frequency changes associated with liquid-solid interfacial phenomena characterizes the energy dissipation as well [18]. This was followed by the development of analytical models for calculating the frequency and dissipation shift applicable to real biosensing by interpreting polymers or biomolecular layers as viscoelastic layers [19]. Prior to that, the main approach has been to interpret the results using the pure mass sensing

approach derived for sensing of infinitely thin rigid layers[20] or by utilizing the theory developed for sensing of infinitely thick liquid media[16]. These two classical limits have subsequently been modified in various ways[21, 22].

Other research conducted on the QCM operation applicable for biosensing includes studies on the influence of surface roughness [23-26], sensitivity and noise in liquid media [27] and interfacial slips [28]. In addition, studies conducted on QCM gas sensing utilizing thick polymer films in view of film resonance[29] and sensitivity amplifications[30] have proven to be of interest also when biosensing with FBAR is concerned [Paper V, VI]. Extensive research has also been conducted into oscillator designs and other driving electronics for QCM in-liquid operation as well as on actual biosensor realizations, but these studies will not be included in the context of this thesis, since the focus is on the actual transducer and transducer principle.

There have further been efforts conducted into enabling interpretations of the sensor response in terms of extracting actual physical properties of the bio-molecular layers, mainly by employing the QCM-D technology [31], by describing the layers as viscoelastic and employing models as the one described above[19]. Further, there are suggestions to extend the applicability of the technology for this purpose by combining the acoustic sensing of the QCM and the optical sensing (SPR or reflectometry) either by comparative studies or by simultaneous measurements.[32-36]

1.3.4 Thin film electroacoustic technology

Whilst the QCM is based on single crystalline bulk material the thin film electroacoustic technology (TEA) is based on the use of thin films (1-3 μm) of polycrystalline materials deposited with IC-compatible processes onto the same type of substrates used for electronic circuits. The operation frequency ranges from few hundred MHz to several GHz.

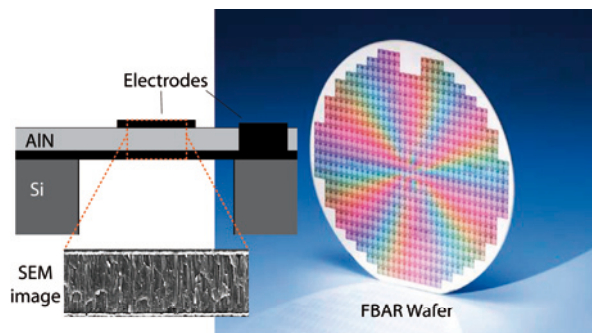


Figure 10. Thin film bulk acoustic resonator (FBAR) fabricated in hundreds onto a Si wafer.

As mentioned above the piezoelectricity requires anisotropy and certain asymmetries to exist, putting requirements on the polycrystalline film to include preferential directional grains.

The commonly used material systems for thin film electro-acoustic applications are the ZnO and AlN wurtzite structures, deposited by reactive sputtering using Zn or Al metal targets respectively. Lead zirconium titanate (PZT) is also commonly used material but often for different applications than here discussed.

The only commercial mass-produced TEA product for high frequency applications so far is the thin film bulk acoustic resonator (FBAR) for filter applications, where the dominating material choice is AlN. The FBAR could be in membrane form as shown in fig. 10 or it can be so-called solidly mounted onto the substrate by using an acoustic mirror underneath. The different topologies will be discussed in section 3.1.

Historic background

FBAR devices first appeared in the literature in the early 1980's [37, 38]. In 1982 Lakin et.al. [39] published a review, which highlighted the potential of FBAR in high frequency low insertion loss filtering and fully integrated oscillator circuits applied for communications and sensors. Zinc Oxide (ZnO) and aluminium nitride (AlN) were identified as the main material candidates.

The early attempts for deposition of thin polycrystalline AlN[40] and ZnO[41] films have been based on the thermal evaporation of aluminum and zinc in a nitrogen and oxygen gas respectively. Chemical vapor deposition for thin AlN synthesis was later introduced for fabrication of single crystalline films for surface acoustic wave applications [42, 43]. Simultaneously there were results reported on reactive sputter deposition of polycrystalline ZnO [44]. And some quite initial results on reactively sputtered AlN films were also reported [45, 46]. Other results were further reported on epitaxially grown ZnO and AlN film using substrates at elevated temperatures (1000-1300°C) with crystallographic surfaces suitable for growth of specific orientations. The techniques reported were reactive sputtering[47, 48] and reactive molecular beam epitaxy [49]. The high substrate temperatures required to obtain epitaxial growth excludes the placement of a metal electrode between the AlN film and the substrate. The latter represented a serious limitation for the practical utilization of such single crystal thin AlN films for FBAR fabrication and underlined the necessity for the development of low temperature process for the synthesis of thin films still having a well defined preferred texture in order to have good piezoelectric performance. Physical sputtering offers a unique means for atom energy control since the energy distribution of the sputtered atoms has a broad maximum at an energy equal to half the sublimation energy of the material, which translates into an equivalent thermal energy in excess of

ten thousand degrees for most materials. By way of example, the surface sublimation energy of Al is 3.36 eV. Using sputter deposition, c-oriented AlN films grown at substrate temperatures not exceeding 500 °C was then demonstrated for the first time on metal [50] and also epitaxial growth onto sapphire could be demonstrated which was prerequisite for the FBAR technology appearing in the beginning of the 80's.

In the early stage of the technology, the non-optimized material quality and the lack of control of the stresses implied a composite design involving support of a Si bridge or in later cases GaN and SiN. With these composite resonators researchers demonstrated: temperature-compensated AlN thickness longitudinal [51] and thickness shear [52] composite resonators. Filters[39] were demonstrated along with longitudinal and shear mode AlN resonators on gallium arsenide [53] operating in the lower GHz frequency band. In addition, monolithic integration of filters on SiO₂ membranes with passive components[54] was demonstrated. The solidly mounted resonator using an acoustic mirror underneath was first reported in 1995 [55]. (The different topologies will be further discussed in section 3.1.)

At this time the early enthusiasm of the technology that had flourished since the beginning of the 80's had settled and there was a notable decrease in published papers for a few years in the mid 90's. In 1998 there appeared reports related to post-processing technique for tuning the resonant frequency [56] and according to Ruby (Avago Technology)[57] it had at that time become clear that a new certain class of filters required by the developments in the mobile phone industry (which should be both compact and have good power handling capabilities) was just that application the FBAR technology could be used for. Substantial capital investments were therefore made in the late 1990's and there has been an ever-growing interest for the technology in the literature since then. In 1999 one of the first free membranes formed of AlN and metal electrode films, without non-piezoelectric support was presented [58]. In 2001 it had reached commercial product; a FBAR based 1900MHz antenna duplexer for mobile phones [59].

The primary manufacturing obstacles of the FBAR were wafer-level packaging and the ability to deposit AlN and metal electrodes with ± 500 ppm (0.1%) uniformity across 6" and 8" substrates [60, 61]. Within the semiconductor industry, film uniformity tolerances are typically a few percent. Today, cellular handset FBAR RF filter and duplexer products are sold containing membrane and solidly mounted FBARs. The FBAR filter technology in general continues to be troubled by yield issues related to film uniformity, which the SAW technology does not suffer from. But the FBAR is anyhow the primary choice when it comes to applications requiring high power and high frequency, which can not be handled by the SAW technology[62].

The new emerging technology of the thin film plate acoustic resonators (FPAR) is combing the IC compatibility of the thin film technology and the

fabrication robustness of the SAW (fewer fabrication steps and less sensitive to thickness variation) at the same time being of high frequency and handling high powers as the FBARs [63, 64]. They do however, exhibit large area compared to FBAR and they require being on a membrane limiting at the present stage somewhat the mechanical stability compared to FBARs. Continuing work is being performed on minimizing the area and further stabilizing the performance by temperature stabilization [e.g. Paper VII].

In conclusion: there has been a growing interest for FBAR since the beginning of the decade driven by the telecom industry and the demand for high frequency filters utilizing longitudinal FBARs with high electromechanical coupling. Film quality as well as electrode material and configuration, were optimized in view of high electromechanical coupling [65], suppression of spurious modes [66] and temperature compensation was achieved [67, 68]. All these efforts driven by the electronics industry generated a well-established technology platform, which can be applied for other types of TEA devices and applications, e.g. sensors.

It is further noted that other applications such as sensors would most likely not be as dependent on film uniformity as the filters, due to different application requirements.

1.3.5 State of the art of the shear mode FBAR technology

Shear mode ZnO and AlN thin film resonators were demonstrated already in the early 80's [39, 53, 69-71] and thin film processes suitable for fabrication of shear mode resonators appeared even earlier in the beginning of the 70's. [69, 72] However, during the strongly commercial driven secondary phase (starting in the late 90's here above described) of the FBAR technology development the longitudinal mode received the primary attention. AlN had become the material of choice due to its mechanical strength and wider chemical compatibility with other required processes and materials in the FBAR structure, e.g. etching selectivity. The large bandwidth requirements of the filters further implied the usage of the longitudinal mode due its strong electromechanical coupling.

The increased interest in biosensors for the anticipated high volume market of point-of-care (POC)⁴ applications in the last decade has been the driving force for continuing the developments of the shear mode thin film technology.

A new original method for the deposition of highly c-textured AlN thin films was developed at Uppsala University [Paper I] without any hardware modifications, heating or biasing. Thereby, fast fabrication of shear mode

⁴ POC analysis refers to the ability to perform diagnostic procedures in a precise and rapid manner at the site where it is needed (i.e. doctors office, on the battle-field or on-site in greenhouses or the field.)

AlN FBAR devices was enabled facilitating testing and evaluation of the device and its potential as a biosensor [Paper II-VI]. Lakin et.al.[38] had also been utilizing a DC planar magnetron system in principle similar to the one at Uppsala University, but in addition an auxiliary anode ring was used which was believed to facilitate tilted growth [70]. They further did not report on any wafer level uniformity.

Simultaneously with the Uppsala developments there was a development at Siemens, Munich, Germany of shear mode ZnO FBARs [73] for biosensor applications [74].

Some other attempts to deposit AlN or ZnO films at low temperatures suitable for shear mode excitation have appeared normally employing a large geometrical tilt of the substrate [75, 76] or by combining this with a grazing incidence ion-beam[77]. None of these studies report on wafer level uniformity.

There have also been attempts to laterally excite the shear mode in c-textured films (usually used for longitudinal modes) demonstrating so far low electromechanical coupling and no realization of biosensor application[78, 79].

Chapter 2

Tilted Film Deposition process

[Paper I]

The development of a deposition process of AlN films with tilted c-axis was essential to enable shear mode FBAR, which is suitable for in-liquid operation. Here a brief description is given on why that is and further also on how such process inhere was realized utilizing conventional sputter equipment without any hardware modifications.

2.1 AlN and the electro-acoustic excitation dependence on the crystalline orientation

Aluminium Nitride (AlN) is a piezoelectric material, primarily used before in the electronics industry as circuit substrates due to its relatively high thermal conductivity in combination with being an electrical insulator. For this purpose it was convenient to have AlN in bulk form.

In its crystal form AlN is piezoelectric having a high stiffness, high acoustic velocity, low losses and rather large electromechanical coupling. Therefore, together with its IC-compatibility, it has become the primary choice for the so far only commercial thin film electro-acoustic device - the FBAR filter. The deposition process of choice is *reactive sputter deposition*⁵. The resulting AlN thin film is *polycrystalline*, consisting of vertical columnar single-crystalline grains packed closely together. Inside each grain, there may exist growth related dislocations, causing some crystallographic planes to shift, but most generally the AlN columns are considered to be single crystalline having one crystal orientation. In order for the total film to exhibit piezoelectric properties the grains need to have the same crystal

⁵ For brief description of sputter deposition see Appendix

orientation along at least one axis of interest i.e. they must have a preferential *crystal orientation* throughout the film.

Crystalline AlN is most often in the Wurtzite crystal structure, which is a hexagonal crystal structure where the Al and N atoms are stacked in a layered AB AB AB structure normal to the c-axis (001 direction), creating a polar axis along the c-axis. Further there is a six fold rotational symmetry around the c-axis. Due to this symmetry the response of the crystal when exposed to external electrical or mechanical force is predominantly determined by how the applied field is oriented relative to the c-axis of the crystal. Fig. 11 illustrates how the electromechanical coupling (defined in section 1.3.2) for the longitudinal and shear modes depends on the angle between the applied electric field and the c-axis of the AlN crystal. It is seen that if the electric field is applied along the c-axis there will be no excitation of the shear mode, but a strong excitation of the longitudinal mode. On the other hand if the electric field is applied perpendicularly to the c-axis there will be excitation of the shear mode but no excitation of the longitudinal mode. The strongest excitation of the shear mode will however occur when the c-axis is tilted about 50 deg from the applied electric field. It is noted that only with the c-axis tilted 90 deg from the applied electric field the mode will be a pure shear mode, otherwise the mode will be a quasi shear mode with a small longitudinal component.

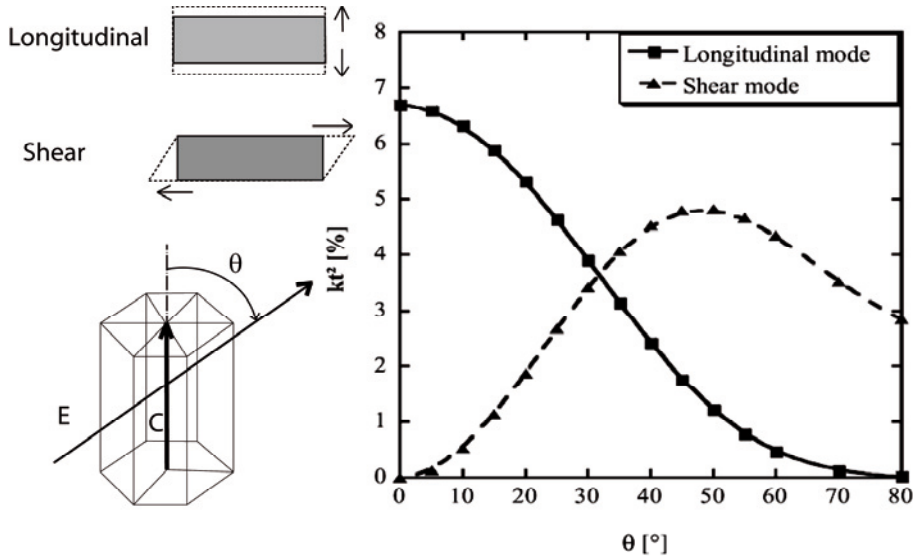


Figure 11. Electromechanical coupling (k_t^2) as a function of the c-axis tilt in hexagonal AlN for the longitudinal and shear mode respectively.[80]

For the layer by layer thin film fabrication technology of thickness excited FBAR it is most suitable to deposit the piezoelectric film evenly onto the

substrate between the bottom and top electrode metal layers creating a parallel plate capacitor (see fig. 12) .

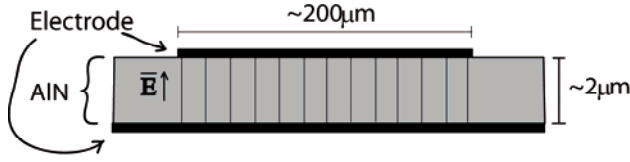


Figure 12. Cross-section of FBAR with electric field lines

Therefore the electric field consequently will be applied in a direction normal to the substrate surface. Hence it is necessary to be able to control the crystal direction of the growth of the piezoelectric AlN film. With the possible liquid based biosensor applications in mind, good efficient excitation of the shear mode would be essential. It was shown that the c-axis needs to be grown tilted at least 20 degrees or more for high efficiency operation in viscous media [Paper V].

2.2 Description of the two-step deposition process for c-axis inclined AlN thin film

The developed reactive sputtering process for growth of AlN thin film with tilted c-axis consists of two steps:

- 1) The process pressure is set high (20mTorr) and an AlN layer of around 100nm is deposited (a so-called seed layer).
- 2) The process pressure is set low (2mTorr) and an AlN layer of around 2-3.5μm (depending on the wanted operation frequency) is deposited onto the seed layer.

The resulting evenly distributed crystallographic tilt is shown below in fig. 13 for a wafer centre symmetrically placed underneath the target. Complete set of process parameters has been published [Paper I] and for more information on the sputtering system see Appendix A.

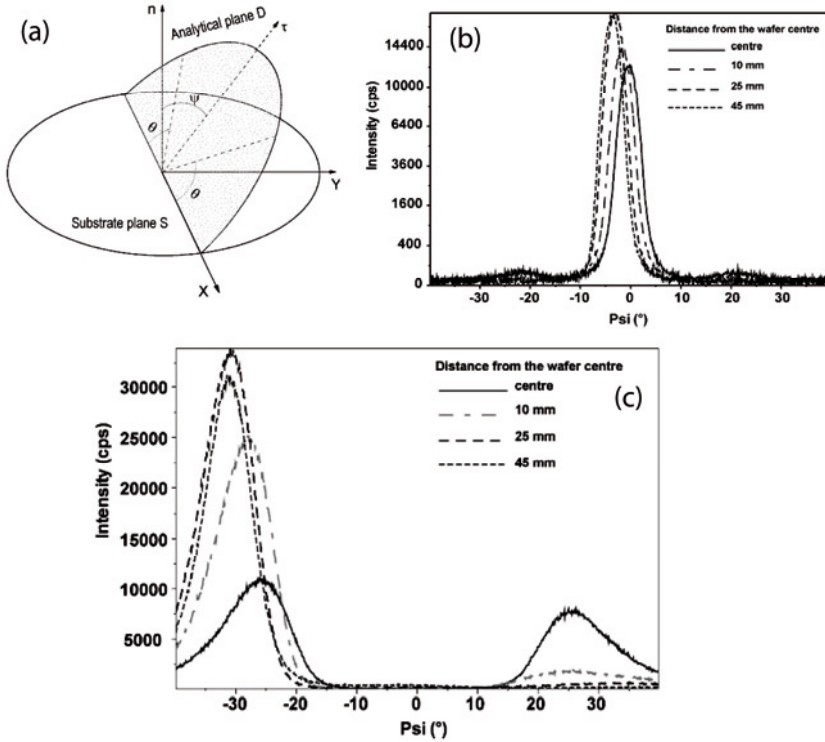


Figure 13. Illustration of the Psi (Ψ) angle in the x-ray diffraction (XRD) setup used for evaluating the tilt of the c-axis. Results are shown on AlN film deposited without seed layer (b) and with seed layer (c). [Paper I]

The tilt of 25-30 degrees will according to fig. 13 enable excitation of both quasi-shear mode as well as quasi longitudinal mode, which have different velocities causing the quasi-shear mode and the quasi longitudinal mode to have different resonance frequencies. Further information on the electrical response of these two resonance modes and their performances in liquid can be found in section 4.2.1.

2.3 Discussion on the tilted film process

In thin film deposition processes a vapor of the material is created thermally, chemically or, as in sputtering, mechanically and then it condenses into a solid onto a substrate. Most generally thin film growth starts with the nucleation of grains on several places on the substrate, so called island nucleation. As these islands grow there will be a competitive growth where the fastest growing islands will consume the slower growing ones. The growth and nucleation of the film is subsequently controlled by the energy, rate and direction of the incoming vapor species and the energy (temperature) of the substrate and its crystallographic structure. The topography of the substrate will also strongly affect the resulting film.

Since the considered process needs to be used on several kinds of substrates often having previously deposited metal layers no external heating is used. This would for many processes indicate that the diffusion rate of adatoms on the substrate is low compared to the deposition rate causing the nucleation to be diffusion limited. This would give islands with similar growth speeds independent on their crystal orientation. Thereby the resulting film would consist of grains with random crystals orientations.

Sputtered species will however have energies high enough to enable high diffusion rates of adatoms even at low substrate temperatures.

At sufficient species and/or substrate energies (that is high enough diffusion rate) it is thermodynamically most favorable that a material condenses onto its most dense crystal plane (the one with minimal surface free energy). In other words, AlN is most likely to nucleate and grow as a (001) grain. That is, the polycrystalline film will grow with the majority of the grains with the c-axis normal to the surface of the substrate.

When the process pressure is high as in the case of the seed layer (20mTorr), the sputtered species will experience multiple collisions lowering considerably their incoming energy and thereby lowering the diffusion rate of the adatoms as well. Thereby nucleation starting on several different crystal planes is enabled.⁶ It has also been seen that such a layer also exhibit larger surface roughness than layer deposited at lower pressures [81].

In the second step of the deposition process the process pressure is low (2mTorr). The sputtered species experience negligible number of collisions in the gas phase and will therefore not loose their energy or directionality. The energy of the incoming species on the substrate will exhibit higher energy and therefore higher diffusion rates than in the first process step. The diffusion is now however strongly limited by the roughness of the seed layer. The roughness of the seed layer could also cause shadowing of the grains facing away from the flux.

It has been seen that the tilt of the c-axis always faces the centre of the wafer and that it corresponds to the direction of the main flux at 2mTorr however the tilt of about 25-30 degrees is much more homogeneous over the wafer than the flux and it corresponds rather well with the 103 crystal plane.

More research is currently conducted into the understanding and optimization of this 2-step tilted film process. The process has proven to be repetitive and controllable for obtaining shear mode FBAR. The process was patented in 2006 [82].

⁶ Calculations concerning the crystal planes of main importance and the angle their normal gives to the c-axis are presented in Appendix B.

Chapter 3

Shear mode FBAR biosensor – design and fabrication [Paper I, II]

Except for the tilted film process presented above and a microfluidic system needed for sensor testing, the design requirements and process steps for the first implementation of a shear mode FBAR biosensor was in many aspects similar to the more conventional longitudinal FBAR. All the process steps need to be IC-compatible and the evaluation of the FBAR requires that it can be electrically connected to a network or impedance analyzer through a GSG-probe from the top side. Several of the issues related to FBAR fabrication can be found in earlier publications and will not be specifically addressed here. For a complete list of the fabrication process steps the interested reader is referred to Appendix C and related references [81, 83]. Here the specific issues related to the implementation of a shear mode FBAR biosensor are presented along with an introduction to the main two FBAR configuration choices; membrane or solidly mounted resonator (SMR).

Further, the realization of temperature stable shear mode FBAR is presented.

3.1 Membrane FBAR versus Solidly Mounted FBAR

In fig. 14 the membrane and the SMR topologies are illustrated.

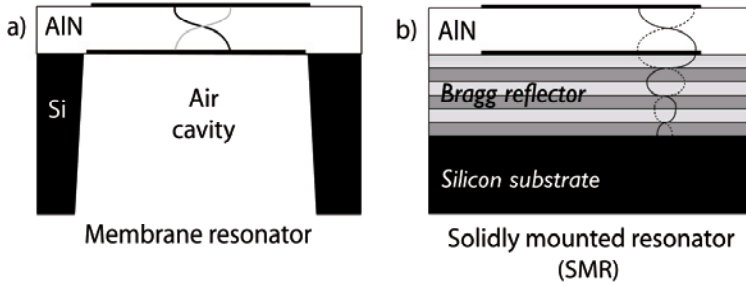


Figure 14. Membrane (a) and SMR (b) type resonators

In the first simplest configuration of the membrane FBAR the acoustic resonance cavity is formed by the creation of an air cavity underneath the bottom electrode by etching partly or completely the Si carrier substrate. One disadvantage of this structure is the substantial decrease of the overall mechanical strength of the supporting Si wafer. To overcome this limitation and to further facilitate the IC compatibility, a surface micromachining process, for formation of a very thin air-gap underneath the piezoelectric film, has been introduced, using sacrificial layers which are etched isotropically.

In the SMR topology the resonator is fabricated on top of a distributed acoustic mirror, a Bragg reflector. The Bragg reflector consists of a sequence of quarter wavelength thick layers of low and high acoustic impedance, respectively. At each layer interface of the Bragg reflector, a part of the acoustic wave energy is reflected. The latter causes the wave amplitude to diminish with depth into the reflector. The number of layers in the Bragg reflector needed for complete wave reflection is determined by their acoustic impedance ratio and the quality of the interfaces.

The SMR provides a more mechanically stable structure than the membrane, but it requires more process and design optimization than the membrane type. For the implementation of the first FBAR shear mode biosensor it was, therefore, concluded that the bulk micro-machined membrane type was the suitable configuration. The membrane type enable manufacturing of a microfluidic channel within the silicon underneath the FBAR for convenient transportation of samples to the sensor surface, i.e the grounded bottom electrode. The latter configuration is advantageous, in that it minimizes parasitic fringe capacitances and dielectric losses.[84]

3.2 Microfluidic channel

The fabrication of the microfluidic channel was realized in one single lithographic and etching step by extending the conventional membrane opening into narrow channels in two opposite directions ending up in circular openings passing through the AlN film. (The complete fabrication flow can be seen in Appendix C.) The anisotropic Si dry etching process utilized to release the FBAR membrane, etches the narrow channels at a lower rate than the larger membrane and circular openings (aspect ratio dependent etching), resulting in the formation of a Si bridge in the channels providing mechanical stability. The bottom of the fluidic channels including the membrane was then sealed with a tape and the fluid was injected through o-ring sealed tubes from the top side. Using a peristaltic pump and an injection valve from Vaccu Inc. for sample exchange a complete microfluidic system was created see fig. 15-17.

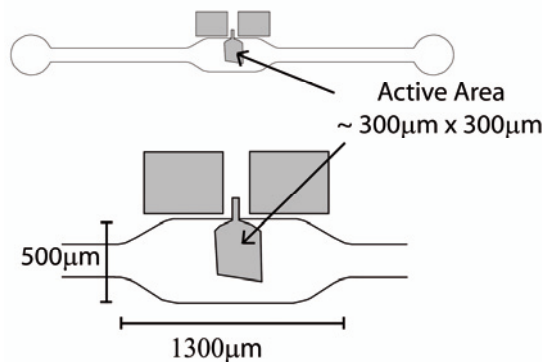


Figure 15. Schematic FBAR biosensor where the fluidic channel is seen beneath the active area.

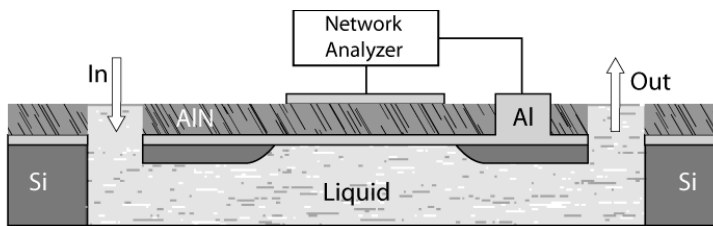


Figure 16. FBAR biosensor in cross section.

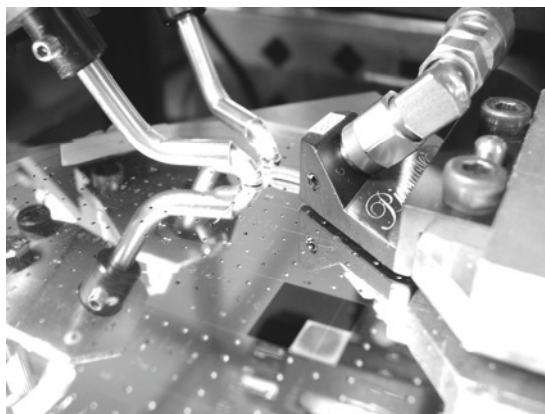


Figure 17. Measurement of FBAR sensor on wafer showing the fluidic channel connectors on each side of the active area.

Since the channel height is determined by the Si wafer thickness and is of the same size as the active area, the effectiveness of the microfluidic channel in terms of mass transport to the sensing surface is low due to its relatively big height. For some applications this could result in long sensor response times and that the full sensitivity of the FBAR may not be fully exploited. This is illustrated in Paper IV. One other disadvantage of the Si fluidic channel is that the sensor surface is inaccessible to the operator. This in turn necessitated that each activation of the sensor surface (biofunctionalization) be done through the fluidic system, and the experiments needed to be adapted and modified accordingly.

These disadvantages along with the mechanical fragility of the membrane indicate that for the future realizations of the FBAR it would be favorable to utilize the SMR technology where the FBAR is solidly mounted onto the substrate and the sensor surface might be activated by imprint or micro-pipette techniques prior to encapsulation. Some applications will however still require that the biofunctionalized surface is kept in the liquid phase. The encapsulation could then be fabricated to create a channel height optimized for effective mass transportation to the sensor surface, using SU8 or PDMS. Such a combined system has been demonstrated using casted PDMS bonded onto a shear mode SMR FBAR, and it demonstrated the possibilities of the above approach but also that further optimization is required to fully utilize the advantages of the membrane technology at this point [85].

3.3 Sensor surface

Finally the in-liquid biochemical sensor requires a suitable surface for biofunctionalization. Traditionally, gold is one of the most commonly used materials. It has proven to be chemically very stable, which is the

prerequisite for reproducible measurements. There are also other materials used as glass and oxides, but since the QCM traditionally uses gold it was convenient to use it for the initial test with the FBAR as well.

Gold is acoustically a high impedance material in addition to having high acoustic losses. Hence, too thick a layer will load the FBAR significantly and at the same time reduce the Q value and the resolution. Conversely, too thin a film exhibits poor surface coverage resulting in poor functionalization. Thus the optimal thickness of the gold film is 20-50nm to ensure full coverage. Successful and reproducible functionalization of the surface necessitates that the Au surface be very clean which implies that gold was deposited as the final step, after the etching of the channel. Au deposition was done with either thermal evaporation or DC sputtering from the backside into the channel onto the Al bottom electrode. Adhesion of gold onto oxidized surfaces commonly requires additional adhesion layer typically a few nanometers of Ti or Cr, which was deposited in situ prior to the gold. This metallization system was successful for measurements in aqueous solutions and was used in all the results here presented.

In the salt solutions that are commonly used for keeping biological molecules, exposed lighter metals such as Ti, Cr and especially Al will however suffer from bimetallic corrosion if in contact with Au. A complete coverage of Au can not always be guaranteed. To be able to create a stable contact as well as a suitable etch stop for the Si-etch, a thin AlN layer was initially deposited before the bottom electrode and used as an etch stop in the deep Si etch. Pt was then used as an adhesion layer prior to the deposition of Au. This metallization system was recently successfully tested for measurements in salty aqueous solutions, but was however not implemented in any of measurements presented in the papers here included.

In conclusion the membrane FBAR with its Si micro-machined fluidic channel created possibilities for fast and convenient testing of the FBAR sensor and was used in all in-liquid results presented within this thesis.

3.4 Temperature compensation of shear mode FBAR

The AT-cut of the QCM guarantees zero temperature coefficient of frequency (TCF) around room temperature giving excellent thermal stability. TCF is defined as the relative resonance frequency shift due to one degree temperature shift. AlN has reportedly a TCF of -25ppm/K, for both longitudinal and shear mode [53]. The TCF depends to some extent on the quality of the AlN film (density, stiffness and stresses).

Temperature compensation of both shear and longitudinal modes in both AlN and ZnO FBARs [51, 86] has been achieved by designing composite resonators containing a layer with a positive TCF to compensate the negative

TCF of AlN or ZnO. Amorphous SiO₂ with its high positive TCF of +85ppm/K is the dominating choice nowadays.

In Paper II a nearly temperature compensated shear mode membrane FBAR is demonstrated with the composite structure of Al/AlN/Al/SiO₂. The temperature dependence of both the longitudinal and the shear mode in the tilted AlN film was studied theoretically and experimentally. The electromechanical coupling and dissipation in view of in-liquid biosensor operation was also studied.

Temperature compensation of the composite resonator is achieved by proper choice of thickness of the SiO₂ compensation layer as illustrated in fig. 18 below.

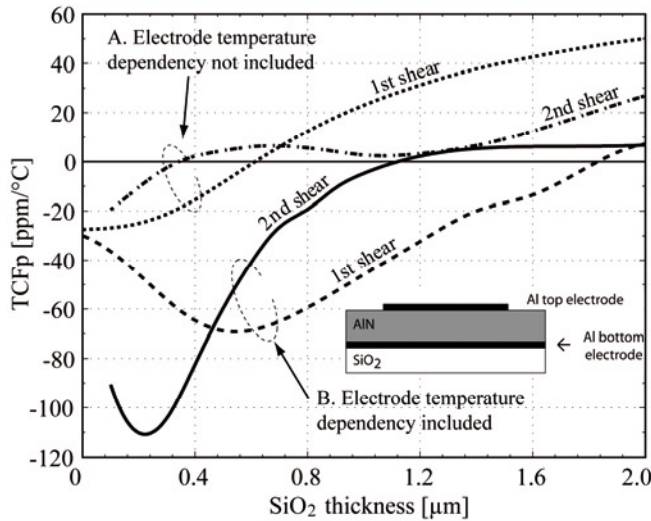


Figure 18. Simulated TCF at room temperature for the 1:st and 2:nd harmonics of the shear mode versus SiO₂ thickness for two different cases; A. The temperature dependence of the electrodes has been omitted and B. when the temperature dependency of the Al electrodes has been included in the simulations. [Paper II]

The lower velocity of the shear mode required that almost twice as thick SiO₂ was added to obtain temperature compensation as in the case of the longitudinal mode. Further, Al does exhibit a rather high negative TCF. Consequently, having an Al layer in the middle of the stack where strain is near maximum will result in that the Al layer strongly affects the temperature behavior of the resonator. Due to the strain distribution, temperature compensation of the Al layers would then require a relatively thick SiO₂ layer despite their small thicknesses.

The fundamental mode is the normal mode of FBAR operation due to its high electromechanical coupling. However, by adding the piezoelectrically inactive material of SiO₂ the electromechanical coupling severely reduces

and more so the more material that is added. When placed with the SiO_2 side in contact with liquid the dissipation increase with increased SiO_2 thickness. It was therefore concluded that in such a shear mode FBAR structure studied it would be beneficial to operate at the second harmonic mode. It was found that operating the resonator in its second harmonic retained in fact its Q value and to a large extent its coupling coefficient. Further, the operation frequency could in this way be retained without reducing the AlN thickness which can result in worse film quality if higher frequencies are desired.

The findings in Paper II were later related to in Paper V where our studies indicated sensitivity of the first harmonic would enhance by adding SiO_2 (despite decrease in frequency). But the higher Q and temperature compensation of the second harmonic would still be beneficial for biosensor operation due to its expected better resolution.

Chapter 4

Shear mode FBAR sensor

– performance and characteristics

[Paper III - VI]

The main part of this thesis is the characterization of the shear mode FBAR sensor in terms of noise, sensitivity and in-liquid performance. The aim of the characterization was to verify, and further develop the shear mode FBAR as a sensor, specifically as a biosensor. Modeling and simulations played a significant role in gaining understanding the operation of the FBAR sensor and how the design parameters influence its performance.

4.1 Noise and resolution

Initial studies with FBAR sensors focused exclusively on the sensitivity amplification that would be gained by the increased frequency of operation and barely addressed the issues related to increased noise and final resolution.⁷ There were concerns that noise levels at high frequencies in GHz region, and small sizes on the micrometer scale, would cause the resolution to be inferior to lower frequency sensors.[87, 88]

It was therefore of significant importance to perform an estimation of the expected resolution of the shear mode FBAR sensor in an early stage of the project in order to establish accurate expectations on the technology.

A sensor exhibits several different resolutions; measurand resolution as well as time resolution. The time resolution will depend on the choice of transducer, but is in many aspects more dependent on the choice of readout. The resolution hereon discussed will be the mass resolution. That is, the smallest detectable

⁷ The influence of the noise level on the sensor resolution has been discussed in the Introduction, where also the difference and relation between sensitivity and resolution has been presented.

change of mass at the sensor surface, when operating in the *pure mass sensor* approximation. The pure mass approximation is valid when the added mass is considered to be ridged, thin and homogeneously distributed on the sensor surface. The resonator frequency is then only affected by the change in mass surface density, independent on acoustic properties (i.e. material) and actual thickness of layer. The mass resolution is then the smallest detectable change of surface mass density. It is further noted that the time resolution will influence the mass resolution by affecting the level of signal averaging, which affects the noise level of the final sensor system.

The mass sensitivity in the pure mass sensitivity approximation is then defined as the relative frequency shift ($\Delta f/f_0$) per changed surface mass density ($\rho_m t_m$), where ρ_m and t_m are the mass density and thickness of the added layer respectively. The sensitivity (S) can then be described by the Sauerbrey equation from 1959 [6]:

$$S = \frac{\frac{\Delta f}{f_0}}{\rho_m t_m} = -\frac{2f_0}{\rho_r v_r}, \quad (1)$$

where ρ_r and v_r are the density and acoustic wave velocity of the resonator respectively. It is noted that here the resonator is approximated to only consist of one homogeneous crystal, thereby neglecting electrodes and other additional layers. This is in many applications a valid approximation of the QCM but will be more limiting in the case of FBAR [Paper V, see below] even though it still will give a fair estimation within the correct order of magnitude. If a noise level [N] is assumed the mass resolution is

$$R = \frac{N}{S}. \quad (2)$$

4.1.1 Electrical Characterization

To design and fabricate FBAR based oscillators at this stage of development would have been severely impractical and time consuming.⁸ In order to evaluate the shear mode FBAR sensor technology on a proof of concept level the measurements were performed on the FBAR using a network analyzer.⁹ Fig. 19 shows schematically the measurement setup employed.

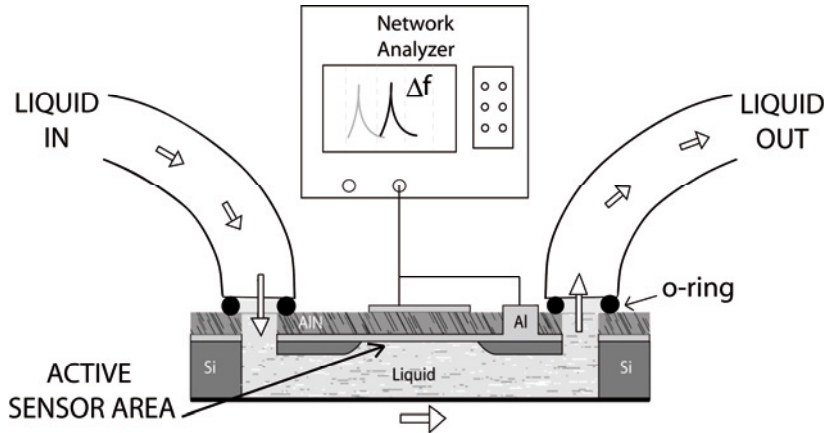


Figure 19. Shear mode FBAR measurement setup.

The network analyzer will measure at discrete points of frequency, which significantly degrade the frequency resolution compared to the actual FBAR. In order to regain some of the resolution, the data was transferred to a computer where a curve fit was implemented to the network analyzer frequency spectra. The series and parallel resonance frequency was then extracted from the maximum of the real part of the admittance and impedance respectively.[89] The Q values for the series and parallel resonance were extracted from the phase (Φ) slope of the impedance and admittance respectively at the series and parallel resonance frequencies (f_i) respectively as:

⁸ Oscillator is one of the conventional, and for QCM the most common, solutions for the electro-acoustic resonator sensor, where the resonator is a part of the circuit, and as the acoustic properties of the resonator changes, the resonance frequency of the whole circuit changes. Another solution is to expose the resonator to an external test signal and determine the resonator response. This can in the case of the FBAR miniaturized sensor be realized with an integrated impedance analyzer.

⁹ A network analyzer is an instrument used to analyze the properties of electrical networks, especially those properties associated with the reflection and transmission of electrical signals known as scattering parameters (S-parameters). Network analyzers are used mostly at high frequencies; operating frequencies can range from 9 kHz to 110 GHz. It is not suitable for final sensor application, but for complete electric characterization

$$Q_i = \frac{1}{2} f_i \frac{\partial \Phi}{\partial f} \bigg|_{max} . \quad (3)$$

The accuracy of the curve fit, instrument performance and the data transferring time limited the sampling time of the sensor measurement to be minimum 10s. The number of measurement points, IF bandwidth and sweep time was set in order to be useful for the majority of the measurements rather than to be specifically optimized for every resonator and measurement.

Noise estimation in liquid

The fluidic channel was filled with water to simulate a biosensor measurement, the difference being that the peristaltic pump was then stopped, minimizing pressure related noise and the formation of unwanted air bubbles. The setup was kept in a normal indoor office environment without any additional mechanical stabilizing or temperature control. The resonance frequency was logged with a sampling time of 10s in the same manor as the sensor measurements were performed. No averaging was applied either within in the network analyzer or by computer calculations afterwards.

The noise level was then calculated using Allan deviation[90] as well as standard deviation. The Allan deviation, which is commonly used with oscillators could however not be performed to the fullest, while the sampling time could not be practically varied. The result has therefore to be considered to be an overestimation of the Allen deviation of the FBAR noise. The standard deviation of the measured fluctuation is a more simple approach and may also be a more adequate measure of the FBAR noise at this stage.

The *first estimation of the mass resolution* using noise thresholds from both the Allan deviation and the threefold standard deviation as well as estimation of the sensitivity based on both Sauerbrey and the NB model yields values for the resolution ranging from 0.3ng/cm² to 7.5ng/cm². This proved the FBAR without any averaging or extra stabilization measures to be on the same level as the conventional QCM (5ng/ cm²) [6] and in some cases even slightly better [Paper III]. It is safe to say that the estimation of the noise performed with the network analyzer is an overestimation and a fair expectation would be that the actual resolution of the FBAR is better than this. Simultaneously estimations were published on the ZnO based shear mode FBAR by Siemens which showed basically the same values [91].

In the final sensor circuit the noise will also be influenced by the noise of the additional devices. The Q-value and the electromechanical coupling (k_t^2), actually the $Q k_t^2$ product, of the resonator will determine the performance of an oscillator. In the following characterizations both the Q and k_t^2 would therefore be of interest.

4.2 In-liquid performance

It is essential for the applicability of the FBAR biosensor that the performance in liquid is of high standard as well as being well defined and controlled.

4.2.1 Verification of the Shear mode

The shear polarisation is the preferred choice for liquid operation of bulk acoustic resonators as well as of plate mode and surface acoustic resonators, since the longitudinal polarisation results in acoustic energy being radiated out into the liquid through compressional motion. This is illustrated in fig. 20 which shows the measured response in both air and pure water of a FBAR resonator made of an AlN film having about 25 degree c-axis tilt. As seen, the quasi-shear resonance retains to a large extent its high Q value whereas the quasi-longitudinal resonance is notably damped when in contact with water.

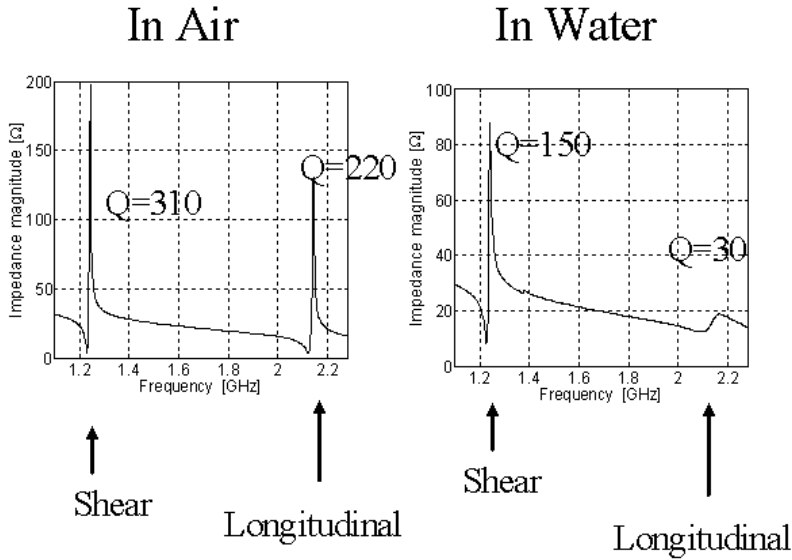


Figure 20. *Electrical response of shear and longitudinal mode resonances in air and in liquid.*

4.2.2 Influence of polarization angle and electromechanical coupling on the FBAR in-liquid dissipation

The shear acoustic wave excited in the polycrystalline AlN film is not a pure mode but a quasi-shear mode. The displacement motion is not parallel to the surface; i.e. perpendicular to the direction of propagation, but has a slight

deviation angle (polarization angle) causing a slight compressional motion in combination with the shear one. Theoretical calculations were performed in order to investigate the actual influence of such a deviation from the pure shear mode on the dissipation the FBAR will experience within liquid media of various viscosities. Fig. 21 shows both the calculated polarization angle and the calculated electromechanical coupling as a function of the c-axis tilt of the AlN film. Further the dissipation due to exposure to water and 75% glycerol respectively was calculated. The simulations assume a bare piezoelectric AlN thickness excited shear resonator with a thickness of $2\mu\text{m}$ and an area of $300 \times 300 \mu\text{m}$ in contact with viscous media.

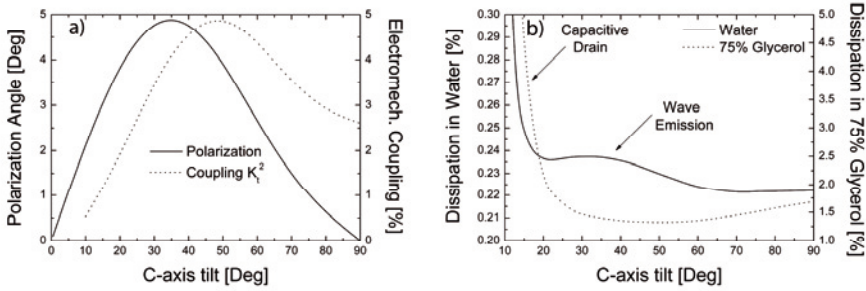


Figure 21. Calculated electromechanical coupling (k_t^2) and polarization angle vs. c-axis tilt (a). Along with calculated dissipation vs c-axis tilt in high and low viscous media respectively (b). [Paper III]

Comparing fig. 21a and fig. 21b it is seen that for liquid media, with viscosity similar to water, acoustic leakage through the longitudinal mode is appreciable for polarization angles larger than 3 degrees (marked with ‘Wave Emission’ in fig. 21b). For media with viscosity much larger than that of water such acoustic leakage losses can be neglected. Much more important in this case seems to be the magnitude of the k_t^2 coefficient. The results are easiest explained by the Butterworth-Van-Dyke (BVD) model¹⁰, where the motional resistance is proportional to the overall motional losses and inversely proportional to the coupling. Substantial increase in the motional resistance, cause a increase in the impedance of the motional arm, which results in even further significant device degradation due to electrical drain through the static capacitance (marked with ‘Capacitive Drain’ in fig. 21b).

¹⁰ The BVD model is an equivalent lumped circuit model of a resonator, describing its electrical response. A so-called ‘motional arm’, describing the electro-acoustic properties of the resonator, is connected in parallel to the static capacitance of the resonator. In an ideal resonator the motional arm will be short-circuited at resonance and hence all the energy will pass through the motional arm.

At low, water like, viscosities the influence of the polarization angle is notable at 30 degree tilt of the c-axis, causing a slightly higher dissipation for quasi-shear mode excited within the tilted AlN film compared to a pure shear mode. At high viscosities the higher coupling achieved with the inclined c-axis film, compared to the pure shear mode, compensates for the losses due to deviation in polarisation angle. On the whole it is concluded that the coupling coefficient has a significant impact on the dissipation at viscosities higher than water and the deficiency due to coupling increases with the viscosity. Further an increase of the c-axis tilt from 25 to 50 degrees (where the coupling is higher) should not theoretically improve notably the dissipation and hence the resolution of the AlN FBAR sensor. A pure shear mode device could be slightly more beneficial at low viscosities, but at high viscosities the dissipation is very similar to the quasi shear mode AlN FBAR with a c-axis tilt of 25degrees.

4.2.3 The Shear mode FBAR utilized as s Biosensor

Shear mode FBAR immunosensor was realized by utilizing antibodies developed for a commercial available QCM based instrument (Biosensor Application AB, Sweden) for detection of narcotics [Paper IV]. The chemistry uses the concepts of competitive binding causing the relatively large antibodies to be released from the sensor surface in the presence of the small target narcotics molecule, causing the mass change to be larger than if the more conventional direct binding approaches would have been used. This approach also guaranteed that the event took place close to the sensor surface, minimizing the influence of the FBAR's shorter detection distance. The response of the FBAR was in many aspects as expected from measurement of the QCM, verifying the applicability of the FBAR for biosensor applications. The slower response for some reactions than in the case of the commercial instrument could be related to the non-optimized fluidic channel and unfavourable mass transportation to the sensor surface.

4.3 Mass sensitivity

The electroacoustic resonator sensing of biological layers in liquid media is complex, where the acoustic path often consists of several layers of non-infinite viscoelastic layers in a viscous environment.

Two very simplified classical limits of the sensitivity can be set up for the system; the first case is when the attached layer is assumed to be very thin and rigid, the so-called pure mass sensing case; e.g. the Sauerbrey equation for the QCM [6] and second case when the resonator is assumed to be in contact with a homogeneous semi-infinite purely viscous medium; e.g. the Kanazawa and Gordon equation for the QCM [16]. For the FBAR, where the

resonator itself consists of several non-piezoelectrically active layers, these two simplified limits will be more complex and need to be addressed specifically for the FBAR case.

It is further noted that the Kanazawa and Gordon equation, mentioned above, is actually derived from the Sauerbrey equation (i.e. the pure mass sensing case) by translating the semi-infinite viscous load limited by the decay length into a pure mass load. The pure mass sensitivity is therefore of fundamental importance for the electroacoustic sensor utilized for biosensor applications as well as of course for other applications, where a mass change at the surface is of interest; e.g. chemical gas sensors.

As described above a *pure mass* load is defined as an added layer where only its mass influences to a first order of approximation the frequency shift independently of its acoustical properties. In general it means that there must be no, or negligible, strain (strain energy) in the layer and that the whole layer moves in phase with the surface of the resonator (no slipping). In addition the wave distribution in the resonator must be unaffected by the added layer. This is fulfilled if the layer has an infinitesimally small thickness, but also if there is a strong reflection between the resonator and the added layer. The latter is fulfilled if low impedance fluids as water like liquids are considered, as in the Kanazawa and Gordon equation.

One striking difference between the QCM and FBAR is the relative thickness of the piezoelectric material in the resonator structure. The thickness of the quartz crystal in QCM is about 300 μm and the AlN layer in FBAR is about 2 μm . The thicknesses of the electrodes are a few hundred nm in both cases, causing a non-negligible portion of the acoustic path in the case of the FBAR to consist of non piezoelectric material. The FBAR needs to be considered as a composite resonator structure.

In Paper V the focus was on the FBAR sensitivity towards negligible thin added layers, which is rigid (no acoustic losses). And further how this sensitivity is influenced by the layers in the composite FBAR structure. Commonly used layers of non-piezoelectric material in the acoustic path of a thickness excited bulk acoustic resonator are the metal electrodes as well as additional layers such as for instance gold (Au, normally used to provide a chemically suitable surface for various biochemical applications), or SiO_2 (used for temperature compensation of resonators based on piezoelectric materials having a negative temperature coefficient of frequency (TCF), e.g. AlN, ZnO). Au and SiO_2 have higher and lower acoustic impedance than AlN, respectively, and are therefore also interesting to use as case study materials for illustrating how high and low acoustic impedance layers influence the sensitivity, respectively.

4.3.1 Theoretical background

The study presented in Paper V is based on the general assumption that in a lossless medium, at resonance, the peak total kinetic energy equals the peak total potential energy in the complete resonating structure, and when adding a layer onto the surface, that energy balance will be perturbed causing the resonance frequency to shift. Further, if the added layer is negligible thin, that frequency change can be used for the determination of the pure mass sensitivity (S) defined as the relative frequency shift $\Delta f/f_0$, normalized to the surface mass density of the rigid thin layer added onto surface:

$$S = \frac{\Delta f}{f_0} = -\frac{(\pi f_0)^2 u_m^2}{U_{Kin}^{Total}} = -\frac{1}{2} \frac{u_m^2}{\sum_{i=1}^N \left(\int_0^{h_i} \rho_i u_i(z)^2 dz \right)} \quad (4)$$

where ρ_m and t_m are the mass density and thickness of the added layer, while u_m is the displacement amplitude in the added layer. It is to be noted that in the case of pure mass sensing the resonance shift is only affected by the mass density and thickness of the added layer and not by its stiffness or other acoustic properties. Hence, the sensitivity (S) will be independent of the choice of sensed material.

The conventional QCM is often considered to be a single material resonator where the structure consists of one homogeneous piezoelectric slab only; i.e. electrodes and other additional layers including the sensed one can be neglected. Under these conditions eq. 4 can be written in a simplified form known as the Sauerbrey equation (eq. 1), where the sensitivity is mainly determined by the quartz slab properties and has the same value independently on which side of the resonator used as the sensing surface.

4.3.2 Mass sensitivity Analysis of Composite resonator structures and sensitivity amplification

From the Sauerbrey equation eq. 1 it is expected that decreased frequency of operation implies decreased relative sensitivity. It was concluded in Paper V that sensitivity amplification could be expected by adding of low acoustic impedance layer even though the resonance frequency decreases. This was concluded to be due to that the relative energy density at the surface increases as a result of the acoustic energy redistribution in a composite resonator caused by constructive interference between the transmitted and reflected waves within the layer.

To prove the correlation both the fundamental and the second harmonic mode of operation will be analyzed for two types of structures: AlN/SiO₂/ambient and AlN/Au/ambient respectively.

4.3.3 Summary of mass sensitivity results [Paper V]

Low acoustic impedance material added to the FBAR will accumulate kinetic energy at the corresponding sensing surface which in turn results in sensitivity amplification at that surface. Experimental measurements agreed well with the theoretical predictions, as seen in fig. 22.

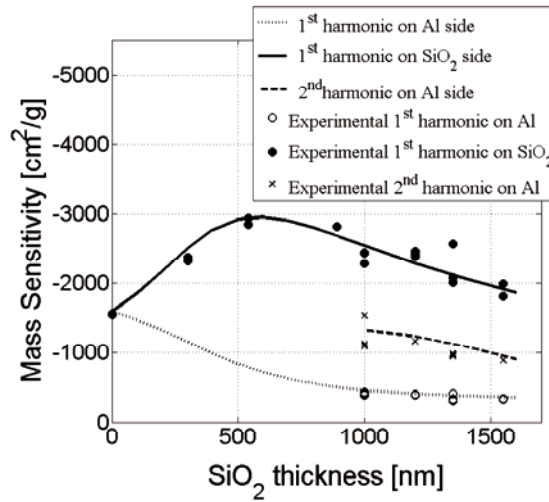


Figure 22. *Calculated and measured relative mass sensitivity for the Al/AIN/Al/SiO₂ FBAR structure for varying thickness of SiO₂. [Paper V]*

In earlier publications, concerning QCM, adding a low acoustic impedance material of sufficient layer thickness has been predominantly done by adding polymer layers for different chemical sensing. Therefore, this sensitivity amplification had earlier been suggested to be attributed to the viscosity of those layers [30]. In Paper V it has however been suggested that the demonstrated mass sensitivity amplification correlates with the reflection and interference of the acoustic waves within the structure, and that it is achieved with any low impedance layer.

Further, since the sensitivity amplification is caused by energy accumulation at the surface, the dissipation in contact with liquids will increase and limit the gain in the final resolution. For the first harmonic mode the added layer will also result in the loss of coupling. Consequently, for high resolution mass sensing in liquids the use of the second harmonic is suggested since temperature compensation in this case is achieved by including a compensating SiO₂ layer while retaining both k_t^2 and Q value

[Paper II]. The sensitivity will in this case be slightly lower, but relatively insensitive to fabrication variations. Further, the dissipation and noise level will be lower as compared to the temperature non-compensated first harmonic.

4.4 Sensing of biomolecular layers and thickness limitations due to film resonance

Modeling of biomolecular acoustic sensing is difficult to perform since the acoustic and physical properties of bio-molecules in generally are unknown. This makes it difficult to predict in a systematic manner the response and limitation of the FBAR (as well as the QCM) since it is directly dependent on the properties of the various biomolecular layers. Even though the QCM has been used for many years as biosensor the actual interpretation of acoustic sensing in terms of the acoustical properties of the layers is relatively unrevealed.

This is not an issue in sensing application when the sensor is calibrated to a known concentration of analyte. Also in analytical applications when affinity measurements are concerned is this often not an issue. For that purpose it is however often important that the sensor response is linear towards concentration of bound analyte.

Applications starting to emerge where the extraction of actual acoustical properties (such as density, elasticity and viscosity) is of interest [32], especially when measurements using the QCM-D equipment are concerned. The QCM-D equipment utilizes measurements of both the frequency shift and the dissipation shift at several harmonics to extract the unknown acoustic parameters including the thickness. It is noted that the parameters extracted will not be related to the bio-molecules only but to the complete layer consisting of the molecules in addition with the surrounding liquid and the so-called *hydration layer*¹¹ surrounding the molecules.

By assuming that the acoustic properties are frequency independent the new QCM-D results [32] make it possible to model predictions on the FBAR response for various molecules. Real measurements will then reveal how well the assumption of the frequency independent properties agrees with the reality, but at least it gives a starting point for what to expect. Here some discussion and illustration on various cases is given along with results from Paper VI.

¹¹ Due to charge-dipole interaction the surrounding water molecules couples to charged molecules. This has claimed to give rise to the higher masses often obtained with the QCM technique than with optical methods like SPR.

4.4.1 Biomolecular modeling

It is common to model the biomolecular layers in the same way as polymers, i.e. as homogeneous layers obeying the Kelvin-Voigt description of viscoelastic materials, in which the complex dynamic modulus (G) can be described as:

$$G = G' + iG'' = \mu + i\omega\eta,$$

where G' and G'' are the storage and the loss moduli respectively. μ is the modulus of elasticity, η is the viscosity and ω is the angular frequency. Further, μ and η are assumed to be real and constant, causing the storage modulus (G') to be constant and the loss modulus (G'') to be frequency dependent. That is the loss modulus and hence the viscosity dependence is expected to be amplified in the case of high frequency FBAR compared to QCM. Below calculations are presented using an analytical model based on the Kelvin-Voigt description. Resonance frequency shift has been calculated (see fig. 23) for QCM and FBAR in contact with a 5nm viscoelastic layer in water environment. The acoustic properties of the layer are set according to reported streptavidin values derived using the QCM-D equipment [32]. It is noted that the reported values from QCM-D measurements reveal that the density of the biomolecular layers are in general very close to water density and the frequency shift is mainly dependent on elasticity and viscosity of the added layer. In fig. 23 the frequency shift is calculated in the parameter space defined by the elasticity and viscosity having values ranging from water up to those reported of streptavidin.

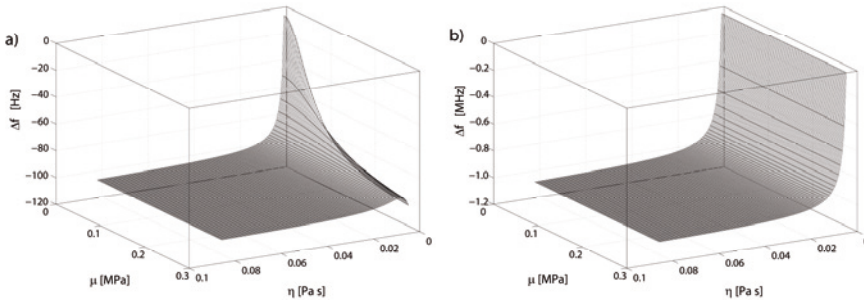


Figure 23. *Calculated resonance frequency shift for 10MHz QCM (a) and 1.5GHz AlN FBAR (b) in contact with a 5nm viscoelastic layer in water environment. The layer density being 1060kg/m^3 and the elasticity(μ) and viscosity (η) ranging from water values to 0.28MPa and 0.082Pas respectively.*

In the parameter space defined by viscosity and elasticity values derived by Larsson et.al. for streptavidin layer [32], it is seen (fig. 23) that the QCM frequency shift depends almost equally on both elasticity and viscosity,

while in the FBAR case the frequency shift depends almost exclusively on viscosity. This would already at this point indicate that by combining FBAR and QCM measurements, new information about the acoustic properties of the biomolecular layers and reaction could be obtained.

4.4.2 Amplitude distribution and effective thickness

To really get an understanding of the sensing in viscoelastic media it is beneficial to study the displacement amplitude distribution in the layers. The acoustic impedance (Z) of the biomolecular layers and the surrounding liquid is very low compared to the solid resonator. AlN ($Z=20\text{MN/s}$) and water ($Z=i*0.1\text{MN/s}$). Therefore strong reflection at the border is assumed causing the amplitude distribution inside the solid resonator to be close to unaffected by the changes in the viscoelastic layers.

In fig. 24 the amplitude distribution for viscoelastic layers with various properties in water surrounding is shown.

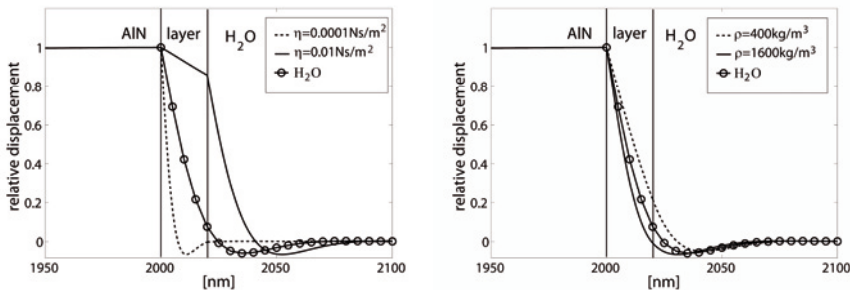


Figure 24. *Calculated amplitude distribution at the moment of maximum strain in the AlN normalized to the amplitude at the AlN surface. The electrodes are here neglected. A 20nm purely viscous layer is placed in contact with the 2 μm AlN resonator. The viscosity and density of the layer is changed according to the inserted legends, the other parameters are set to those of water.*

Here the general statement is presented that in the case of any strained low acoustic impedance film of physical thickness t it can be transformed into the case of pure mass-loading (un-strained film) by using an *effective thickness*. Within this effective thickness the displacement amplitude is considered to be homogeneous, in phase and equal to that at the piezoelectric crystal interface. Note that to completely translate the problem into pure mass-sensing, the wave distribution inside the resonator must still be considered to be unaffected; i.e. there must be strong reflection at the border.

The effective thickness **d** is defined as the thickness that will give the same flow rate with constant velocity as the actual velocity distribution as:

$$dv_0 = \int_0^{t_m} v dy ,$$

where v_0 is the displacement velocity at the solid resonator surface and v is the velocity distribution inside the layer.

It is from fig. 24 concluded that high viscous layers will have larger effective thickness than low viscous layers. That is, more of the high viscous layers will be sensed than the low viscous layers. The high viscous layer will also sense the bulk liquid more since the acoustic wave is not that fast attenuated as in the low viscous case. It is further seen that a high density viscous layer will have a smaller effective thickness than a low density viscous layer. Thereby it is concluded that there could be layers with the same physical thickness but different densities exhibiting the same effective mass (the effective thickness times the density and area) and hence give the same frequency response.

The amplitude distribution in the layer will depend on the inference of the reflected waves in the structure, which is strongly dependent on thickness. In fig. 25 the amplitude distribution in water layers of various thicknesses are seen .

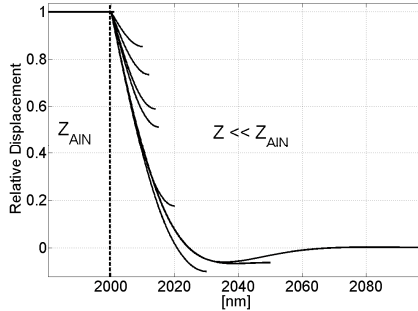


Figure 25. *Normalized displacement amplitude distribution calculated for the first harmonic pure shear mode at the moment of maximum strain in the AlN for a 2 μ m AlN resonator, with imaginary thin electrodes on each side with an additional layer of water with varying thicknesses on one side. The displacement amplitudes are normalized to the amplitude at the free AlN surface.*

4.4.3 Film resonance

It is seen in fig. 25 that the amplitude distributions are flatter for thinner layers and that they do not follow the distribution of the semi-infinitely thick

layer. The effective thickness for each layer can be placed as the thickness in the Sauerbrey equation and the frequency shift can then be extracted accordingly. The results for such effective thickness calculations can be seen in fig. 26 along with calculations using the analytical model of Voinova and Nowotny-Benes calculations. Good correlation between these three models is clearly shown.

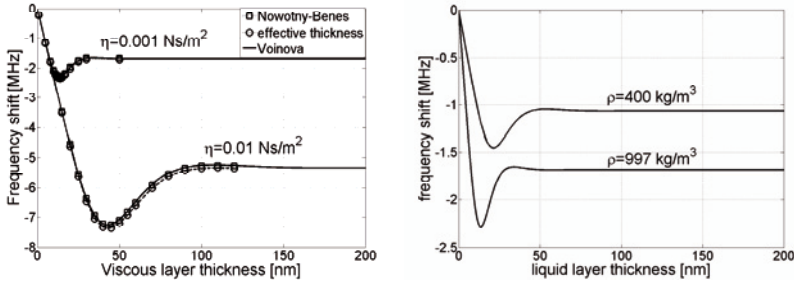


Figure 26. Calculated frequency shifts, for two $2\mu\text{m}$ composite AlN resonators operated in air having imaginary thin electrodes and each having an additional liquid layer of varying thicknesses on one side. The two liquid layers have varying properties as described in the figures. The other properties are equal those of water.[Paper VI]

Fig. 26 clearly shows a non-linear frequency dependence on the layer thickness. Fig. 26 indicates a point of maximum frequency shift and accordingly maximum effective layer thickness. After this point there is a reversed (positive) frequency shift after which its absolute value decreases steadily to finally saturate as a function of layer thickness. Adding the effect of the surrounding bulk liquid often present in bio-sensing application will affect somewhat the frequency shift behavior seen in fig. 26. In addition, the inclusion of a limited elasticity will further affect the level of the saturated frequency shift for thick layers, although not so much the position of the maximum absolute frequency shift. This reversed frequency shift Martin et. al. earlier introduced to be caused by the film resonance for thick viscoelastic polymer films on QCM, which occurs in the vicinity of a phase shift of $\pi/2$ (that is layer thicknesses of $\lambda/4$).[29] Around this thickness the constructive interference of the waves inside a low acoustic impedance layer is the strongest, causing the effective layer thickness to be the largest. Note that in the region of positive frequency shift the sensor might also respond with a positive frequency shift to a small increase in layer density, therefore, unaware operation within this region could result in serious misinterpretation of the data.

Even though the concept of effective thickness gives a fairly good visualization of the phenomena of film resonance, it is most commonly

described by the acoustic impedance. The input acoustic impedance (Z) of a layer in contact with vacuum is described in the transmission line model by:

$$Z = iZ_0 \tan(\beta),$$

where the Z_0 is the acoustic impedance, which is the density times the acoustic velocity, and β is the acoustic phase shift across the layer. It is clearly seen that a singular point will occur when β approaches $\pi/2$ that is layer thicknesses of a quarter wavelength. At this point the constructive interference between the transmitted and reflected waves within the layer causes the input acoustic impedance to increase infinitely. In the case of biosensor applications the viscous damping within the bio-molecular layer as well as due to the surrounding liquid media will strongly limit the singular point resulting in a well defined, but non-linear frequency response.

It had been suggested that the higher frequency of the FBAR and hence faster *decay* of the acoustic wave in viscous media would limit the thickness of the bio-molecular layers that could be used for biosensing. In Paper VI it was, however, found that a stronger limitation of the linear sensing regime would be imposed by the *film resonance*.

In Paper VI both theoretical and experimental investigations of the frequency shift versus thickness of biomolecular viscoelastic layer are done. The frequency decreases linearly with layer thickness for thin layers until reaching a maximum at around film resonance. Increasing the film thickness further results in an increase of resonance frequency until saturation is reached after which the resonance frequency is insensitive towards layer's thickness. In paper VI it is shown that the film resonance does, as expected, occur at considerably smaller thicknesses of the added layers than in the case of QCM, but that the thicknesses at which the point of reversed frequency shift for the protein systems studied occur is larger than many of the molecular systems intended for FBAR biosensor applications.

Chapter 5

Lamb mode waves and devices

[Paper VII]

In a FBAR device there is excitation of lateral field excited (LFE) modes as well as thickness excited (TE) modes earlier discussed. The LFE modes in FBARs mostly consist of laterally propagating guided plate modes (also known as Lamb waves), which undergo reflections from the electrode edges and can thereby form a number of unwanted spurious resonances in the vicinity of the main resonance.

These LFE modes are therefore mainly seen as unwanted spurious modes in the case of TE FBAR devices. There are however devices utilizing these modes. Inhere, we discuss one such Lamb mode device [see also Paper VII]. However, a general description of the Lamb modes and their influence on the different configurations of FBARs will first be given.

5.1 Lamb modes¹²

Lamb waves are guided *plate waves*. Their particle motion lies in the plane defined by the plate normal and the direction of wave propagation. Another type of plate mode wave is the *shear plate mode* whose particle motion is orthogonal to the direction of wave propagation and in the plane of the plate.

Generally the plate mode is supported in plates of the same order or smaller thickness than the wavelength. As the relative plate thickness grows larger the acoustic energy will be more and more accumulated to the surface hence generating *surface acoustic waves*.

¹² Lamb modes are named after the English mathematician Horace Lamb [1849-1934].

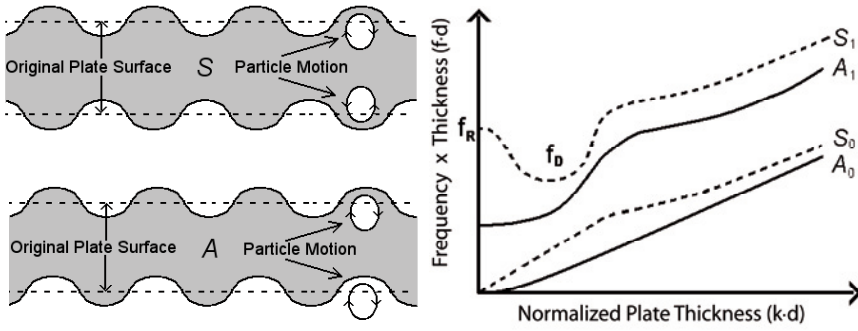


Figure 27. Illustration of the particle motion in the Symmetric and Anti-symmetric Lamb modes. Dispersion of the first few Lamb modes as a function of the relative plate thickness. Note that the wavenumber (k) is in the plane orthogonal to the plate thickness.

There are two different Lamb mode types. These are the symmetric and the asymmetric modes respectively indicating the symmetry of the particle displacements associated with the wave relative to the median plane of the plate (fig. 27). For simplicity the different plate modes are denoted with symbols. Thus the n^{th} order symmetric Lamb wave is denoted as S_n , the n^{th} order asymmetric Lamb wave is denoted as A_n , where "n" is an integer ranging from 0 to infinity. Figure 27 shows the typical dispersion of the first few Lamb modes as a function of the relative plate thickness.

At the cut-off frequencies of S_1 and A_1 , the modes have zero lateral wavenumber k , which are exactly the shear and longitudinal thickness excited modes respectively as represented by the one dimensional model used for FBAR.

5.2 Lamb modes in FBARs

Two effects need to be considered when unwanted Lamb mode excitation in FBARs is concerned. First, as mentioned above the spurious modes arise from laterally propagating modes which are in turn trapped in the resonator cavity by reflection at the electrode edges resulting in degradation of the resonance response. The second effect is the energy leakage out from the resonator cavity due to coupling to lateral propagating modes outside the cavity, which degrades the Q-value.

Spurious response

The spurious resonances caused by the laterally propagating modes in FBARs have been suppressed by designing electrodes with an irregular geometry, that is, with non-parallel edges. This technique is also called "apodization" [92] and ensures destructive interference between the lateral

modes reflected from the electrode edges. An extension of this technique has been proposed in [93] where electrodes of elliptical shape have been employed. Another competitive approach is designing a narrow border region, placed in-between the active and the outside regions, in a way to ensure continuity of the vertical displacement and its corresponding strain between the both regions for SMR [94] and membrane [66] based FBAR. The latter technique is thought to cancel the reflection at the electrode edges.

Energy leakage

By plotting the dispersion curves in fig. 27 in absolute frequency scale it can be seen which type of mode transformations that are possible in membrane FBAR structures. The acoustic modes can only couple to modes having the same or very close frequencies. Generally the cut-off frequency of the region outside the resonator area is higher in comparison with that inside the resonator. Therefore the curves representing the outside are placed slightly above the ones representing the inside of the FBAR cavity. It is then concluded that the thickness excited shear mode (placed at the cut-off frequency of the A1 mode) can only couple to the S_0 and the A_0 modes with rather high wave-numbers. This coupling is not very strong and therefore it is expected that the shear mode FBAR cannot couple strongly to lateral propagating modes outside the resonator. The latter prevents energy radiation out of the resonator. On the other hand the longitudinal mode (placed at the cut-off frequency of the S1 mode) can actually easily couple to the S1 mode with a rather low wave number. The longitudinal mode can also couple to the A1, S0 and A0 modes, but not that strongly.

It is noted that fig. 27 illustrates the dispersion curves in free plates, which also corresponds to membrane type FBARs but not SMR type FBAR. The properties and the dispersion of the laterally propagating modes are somewhat different for the SMR type FBAR. Generally, due to mechanical stiffening of the plate the dispersion of the S1 mode is such that the longitudinal mode cannot couple strongly to laterally propagating modes outside the resonator as in the case of membrane type FBAR. However, there can be leakage through these modes into the reflector underneath the resonator. The reflector can in turn be optimized to be reflective for some of these modes and thereby improve the Q [95].

5.2.1 Lamb modes in c-axis inclined AlN FBAR

In the case of c-axis oriented AlN plate there is a high symmetry in the plane orthogonal to the plate thickness (in the case of polycrystalline AlN there is full symmetry). Thereby the excitation of the laterally propagating plate waves will be equal in all direction implying that the excitation and suppression of the spurious modes will be independent on how the electrode edge is oriented.

This symmetry is broken in the case of the quasi-shear mode FBAR based on c-axis inclined AlN. The quasi-shear polarization lies in the plane defined by the plate normal and the c-axis tilt vector. It is, therefore, expected that the A1 mode is coupled in this direction, while the shear plate mode is coupled in a direction orthogonal to the plane of polarization. Further, the A1 and the shear plate modes have different velocities generating a non-symmetric velocity profile. The suppression and excitation of the spurious modes could, therefore, be dependent on the electrode geometry and orientation in a different manner than the so far mainly studied c-axis oriented AlN. This issue has however not been studied in the context of this thesis.

5.3 Lamb mode devices - Thin film plate acoustic resonators (FPAR)

Thin film plate acoustic resonators (FPAR) usually utilize the low dispersion range of the S0 Lamb mode. It offers low sensitivity towards fabrication process variations, i.e. small film thickness variations. Because even though Lamb modes are generally dispersive, the lowest order symmetric Lamb wave (S0) is low dispersive for relative thin plates as seen in fig. 27. Fig. 28 shows the velocity for the S0 mode versus film thickness normalized to the wavelength (d/λ), and clearly illustrates the low dispersion of the S0 mode at small relative thicknesses.

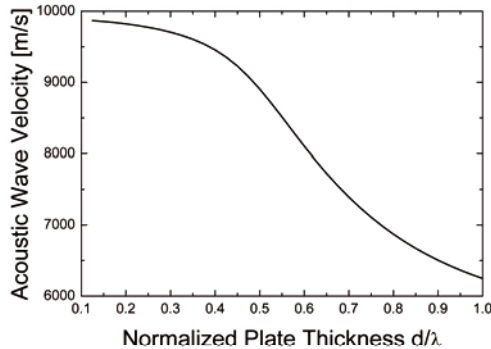


Figure 28. *The acoustic wave velocity of the lowest order symmetric Lamb wave (S0) plotted versus AlN plate thickness (d) normalized to the acoustic wavelength (λ).*

FPAR configurations

Thin film plate acoustic resonators (FPAR) are generally Lamb mode devices where the Lamb mode is excited by interdigital transducers (IDTs).

The periodicity of the grating is related to the wavelength of the excited wave. To create a resonating cavity the lateral wave thus generated is then reflected on either side of the transducer by suitable reflectors. FPARs are being developed in two different topologies with respect to the acoustic wave reflection. The first one is based on the reflection from the suspended free edges of the thin plate [96-98], while the other is based on the reflection from distributed reflectors represented by a periodic grating with a grating pitch of a half wavelength [99, 100].

There exist two major transducer geometries. The first one is a standard IDT (Figure 29a), while the second one represents a periodic strip transducer with an additional bottom electrode (Figure 29b,c).

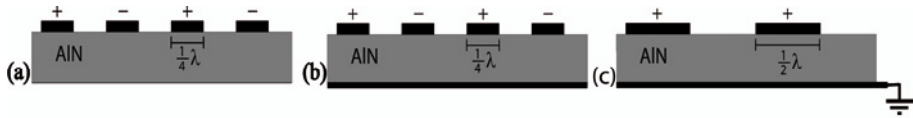


Figure 29. Lamb wave excitation geometries of practical interest; using IDT electrodes without metal layer underneath (a), using IDT electrodes with metal layer underneath at floating potential (b) or using a bulk transducer with grounded metal layer (c).

It is noted that in the latter case the electric field is oriented predominantly in the vertical direction, thus giving rise to lateral field excitation of modes with longitudinal polarization through the e_{31} piezoelectric coefficient. These transducers we call longitudinal wave transducers utilizing a lateral field excitation (LW-LFE) as previously suggested [100]. At relatively small-normalized plate thicknesses the LW-LFE transducers offer much higher electromechanical couplings as compared to the standard IDT configuration. The latter yields, in general, lower but still acceptable couplings, but on the other hand requires fewer fabrication steps. Both types of transducers have been demonstrated in high Q FPARs and their potential discussed [100]. Further, it is noted that theoretically the highest electromechanical coupling should be obtained if the bottom electrode is patterned in the same manner as the topside gratings generating a symmetrical structure. This will, however, generate fabrication issues such as cracks in the subsequently deposited AlN. This could be avoided by buried-electrode approach [101], but this is at the moment not seen as a practical approach for mass fabrication.

FPAR background

The development of acoustic resonators operating in the lower frequency (0.5 MHz – 5 GHz) band as well as the development of other types of thin film electroacoustic devices (as for example delay lines, longitudinally coupled filters, sensors, two-port resonators etc.) is a challenging problem of great importance and potential. SAW and BAW are the two major types of

waves employed. BAW is represented by the FBAR at frequencies from 1GHz and above. Full process integration between the FBAR technology and the IC technology is possible, but yield issues related to stringent requirements on metrology, thickness uniformity and the high number of fabrication steps needed still persist.

The SAW technology based on single crystalline substrates is by definition incompatible with IC fabrication, but there are less stringent requirements on metrology and thickness uniformity. The number of fabrication steps needed is also far less than for FBAR. The central frequency of a SAW device is determined by the equation $f = V_{\text{WAVE}}/\lambda$, where f is the resonance frequency, V_{WAVE} is the phase velocity of the acoustic wave and λ is the acoustic wavelength, which in turn is defined by the electrode pitch in the inter-digital transducer (IDT). Hence, high-resolution lithography and/or the use of high acoustic velocity materials are the two main approaches for the fabrication of high-frequency SAW devices. The first one, however, results in an increased fabrication cost while the second one is limited to the choice of commercially available piezoelectric materials. The conventional SAW technology has at the present state an upper frequency limit of about 1-2 GHz.

The latter inspired a number of studies on high velocity surface acoustic waves (HVSAW). A thin piezoelectric film is combined with a high-velocity non-piezoelectric substrate thus providing a flexible platform for high frequency SAW devices. The high velocity non-piezoelectric substrate is usually sapphire or diamond. The disadvantages of the HVSAW concept include the relatively high cost and increased losses emanating from the defects induced at the interfaces. Further, it is not a practical for full integration.

The utilization of laterally propagating fast wave-guided modes known also as plate waves in thin AlN membranes (FPAR) has recently been demonstrated [102, 103] as a promising alternative to the HVSAWs. The full potential of FPAR still needs to be further investigated with respect to electromechanical coupling optimization and area minimization. In Paper VII temperature stabilization in view of optimized electromechanical coupling is demonstrated.

5.4 Temperature stabilized FPAR

Due to the non-zero temperature coefficient of frequency (TCF) of AlN, the FPAR device needs to be temperature stabilized analogously to the FBAR. And as in the FBAR case one approach is to temperature compensate using SiO₂. This approach is demonstrated in Paper VII. Such a temperature compensated structure is schematically shown in fig. 30 in its simplest configuration, which is without bottom electrode. It is noted that inclusion of

bottom electrode would improve the coupling but not change the principle of the temperature compensated behavior presented in Paper VII.

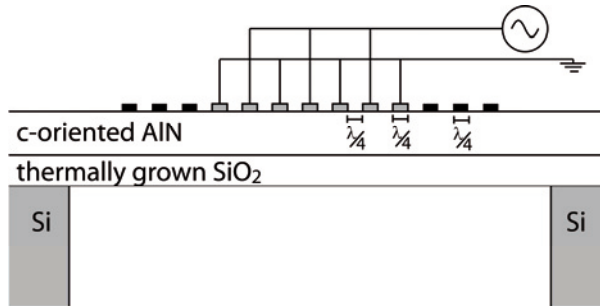


Figure 30. Topology of the thermally compensated FPAR

The temperature compensation was studied theoretically as well as experimentally. Experimental results on the temperature dependence of the resonance frequency are shown in fig. 31 for three different SiO₂ thicknesses.

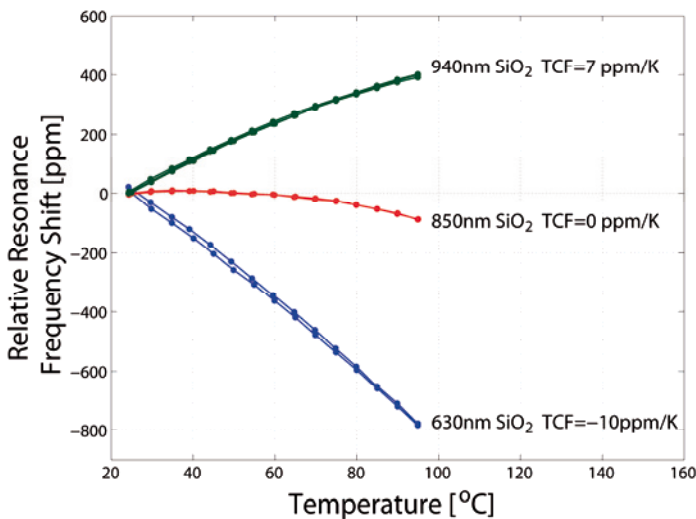


Figure 31. Resonance frequency shift relative to resonance frequency at 25°C measured for synchronous devices on AlN/SiO₂ membranes with varying SiO₂ thicknesses in the temperature range of 25 to 95°C. The presented TCF values are calculated in the vicinity of 40°C. The thickness of the AlN was always kept at 2μm and the wavelength at 12 μm.

The TCF values in fig. 31 represent the linear temperature coefficient of frequency. In many real applications it is also important to minimize the second temperature coefficient of frequency. From the measured data using 850nm SiO₂, the second order temperature coefficient of frequency is found

to be $\beta = -31 \text{ppb/K}^2$. For comparison the second order temperature coefficient of frequency demonstrated inhere is larger than that for temperature compensated AlN FBAR ($\beta = -20 \text{ppb/K}^2$) [104] but smaller than that for SAWs on ST-cut quartz ($\beta = -34 \text{ppb/K}^2$) [105].

In Paper VII comparison between different designs concerning excitation and reflection is also presented along with a discussion. It was found that temperature compensated asynchronous¹³ FPAR devices exhibit higher Q and smaller size in comparison with their synchronous¹⁴ counterparts.

¹³ 'Asynchronous' is here used for devices having a cavity length of $(n + 1/2) \lambda/2$. The design of the transducer and the position of the reflectors are done in such a way to move operation frequency into the centre of the passband.

¹⁴ 'Synchronous' is here used for devices having cavity length of $n\lambda/2$ and operates at the upper stopband edge.

Chapter 6

Concluding remarks and Further Discussion

The main strength of the FBAR technology is its full compatibility (both fabrication and functional) with the IC technology enabling mass production of miniature sensor systems especially arrays. So it is not until a complete biosensor system is developed that the true potential of the FBAR technology can completely be revealed. A biosensor in general consists of several units such as sample collection, fluidic channel system, biomolecular recognition element, transducer, driving electronics and read out circuitry. The complexity of such a system requires that all the units be integrated and such integration requires a lot of dedicated engineering and research involving expertise from diverse fields of science and technology. Because of the amount of money, time and expertise investments required it is essential that the potential for each separate unit is well established in view of the final application before starting the final integration.

This thesis has been focusing on the performance and operation of the actual shear mode FBAR transducer in view of biosensor applications. The results of this thesis have strengthened the prospects for shear mode FBAR based biosensors. The early apprehension about for example unacceptable low performance of the high frequency FBAR due to the expected high noise level has been strongly contested. Mass resolution has been demonstrated to be of the same order if not better than that of oscillator based QCM sensors. With respect to transducer performance the main competitive technique is the conventional QCM system in view of the same transduction principle used.

Even though the FBAR transducer is similar to the QCM there are some major differences. The much higher frequency and smaller size put focus on issues and effects, which in many cases are considered to be negligible when using QCM, and therefore often ignored. It is important to note that with the FBAR, where the effects are significant, these issues are highlighted and hence provide additional understanding to the operation of all bulk shear

mode electroacoustic devices, including the QCM. In addition, the knowledge of the biological layers properties could be improved by letting the FBAR's higher frequency provide complementary data to the measurements done with QCM.

Possible applications for the FBAR biosensor could be divided in the same two categories as the QCM biosensor; i.e. actual biosensor applications and analytical tools. While the dominating use of the QCM sensor seems to be for analytical purposes, the mass fabrication technology¹⁵ of the FBAR device makes the FBAR more suitable for mass market application like point of care applications.

The FBAR technology has made it possible to move the thickness excited shear mode sensing of biological layers into a new sensing regime using substantially higher operation frequencies than the QCM. Therefore there are also as mentioned above reasons for utilizing the FBAR for analytical research purposes as well.

6.1 Findings

The main results of this thesis concerning the FBAR sensor applicability, performance and fabrication are presented in summary below.

1. [Paper I] A two-step IC-compatible deposition process has been developed using conventional sputtering equipment to deposit thin AlN film with a tilted c-axis of 20-30 degrees on a broad variety of substrates.
2. [Paper III] It was concluded that the tilt of the c-axis should not be below 20 degrees to ensure high effective shear mode operation and to avoid capacitive drain.
3. [Paper III] It was concluded that even though stronger excitation of the quasi-shear mode could be expected at large c-axis tilts the dissipated energy for viscosities equal to that of water value or higher would be in principle the same, independently on c-axis tilt for tilts higher than 20 degrees.
4. [Paper I] This AlN sputtering process was used for fabricating shear mode FBARs operating at above 1GHz showing Q values of 100-200 in water and electromechanical coupling factors k_t^2 of about 1.8%.
5. [Paper IV] The suggested microfluidic channel integrated in the Si substrate underneath the membrane FBAR was demonstrated to be adequate for testing the sensor. There were, however, certain drawbacks with this fluidic channel system.

¹⁵ Mass fabrication technology usually applies for fabrication technologies which do have fairly large start up costs but then have low fabrication costs per unit if the number of units exceeds a critical amount.

6. [Paper IV] The shear mode FBAR was demonstrated as an actual immunosensor for the detection of narcotics.
7. [Paper II] A temperature compensated shear mode FBAR composite structure was demonstrated with retained coupling factor and Q-value by utilizing the second mode of operation.
8. [Paper III] Measured noise level of shear mode FBAR in contact with water showed the resolution to be in the range 0.3ng/cm^2 to 7.5ng/cm^2 . This was the first demonstration of the FBAR resolution without any averaging or extra stabilization measures showing unequivocally to be already in the same range as the conventional QCM (5ng/cm^2).
9. [Paper V] While the thickness and influence of electrodes and other non-piezoelectric material layers can often be neglected in the case of QCM, the FBAR structure in its simplest case consists of 15% of non-piezoelectric materials. For temperature compensated devices up to half the thickness represents non-piezoelectric materials. When it comes to estimate the influence of the non-piezoelectric materials in the multilayer FBAR structure the classical understanding tells us that adding more material in general to the resonator will lower the resonance frequency and increase the total mass and hence decrease the mass sensitivity.
 - a. The classical Sauerbrey equation was shown to give an estimate of the mass sensitivity to an order of magnitude. Therefore, it could easily be used for rough comparisons between FBAR and QCM.¹⁶
 - b. Contrary to standard understanding, however, it was found that by adding non-piezoelectric material of low acoustic impedance to an FBAR resonator operated in its first harmonic the sensitivity could actually be increased by as much as a factor of 2 even though the frequency subsequently decreased while increasing the total mass.
 - c. By adding non-piezoelectric material of high acoustic impedance to an FBAR resonator operated in its first harmonic the sensitivity decreased as expected according to the classical understanding.
 - d. By adding low acoustic impedance electrodes such as Al the sensitivity was increased somewhat according to b) and then by placing high acoustic impedance layer of for instance Au onto the Al the sensitivity was increased even further.
 - e. The amplified mass sensitivity seen was always accompanied with higher dissipation in contact with liquids.

¹⁶ The FBAR was then approximated into only consisting of one homogenous piezoelectric slab in the same manner as the QCM.

- f. The trend in b) and c) was reversed in the case of second harmonic resonators.
 - g. b)-f) could be explained by studying the amplitude distribution inside the multilayer structure and the increased sensitivity could be related to accumulated energy at the surface due to constructive interference of the reflected waves.
10. [Paper VI] The linear thickness limit for sensing of biomolecular layers was concluded to be larger than the thickness of the majority of the molecular systems envisaged for FBAR biosensor applications.
 11. [Paper VII] Temperature compensated Lamb mode (FPAR) devices were demonstrated with well retained electromechanical couplings.

Chapter 7

Sammanfattning på svenska

Utvecklingen mot allt mindre enheter pågår både för elektroniska komponenter och sensorer. Kombinationen blir spännande. Inom de medicinska sensortillämpningarna kan det till exempel leda till minskade kostnader då det är betydligt billigare att använda masstillverkade chip istället för traditionell provtagning. Inom biomedicinen sker det idag stor utveckling inom patientnära lösningar, dvs. metoder som inte kräver specialistkompetens och som gör det möjligt att utföra diagnosen direkt på den lokala vårdcentralen eller till och med i hemmet av patienten själv. Med hjälp av så kallade biomarkörer ska man med ett enkelt blodprov kunna identifiera t.ex. cancer utan kirurgiska ingrepp.

En sådan utveckling mot mer patientnära lösningar skulle kunna avlasta det nuvarande vårdsystemet samt göra det möjligt för snabbare diagnostik och kortare vårdköer. För att en allmän och bred spridning av ett patientnära vårdsystem ska vara möjlig krävs miniatyriserade och billiga sensorlösningar.

Där måste dessutom finnas möjlighet att övervaka informationsflödet från dessa sensorer. Framstegen inom elektroniken de senaste decennierna har gjort det möjligt att hantera och behandla stora mängder data. För att kunna åstadkomma ett komplett och användbart nytt vårdsystem krävs det att sensorerna kan övervakas elektroniskt och vara lätt integrerbara med den datorbaserade teknologin.

En biosensor är ett analytiskt verktyg där man utnyttjar det faktum att det i biologiska system finns molekyler med överlägsen förmåga att specifikt reagera med olika analyter, dvs. molekyler som man avser utföra bestämning av i ett system. Biosensorer används inom många olika områden från medicinsk diagnostik till processövervakning i läkemedelsindustrin och detektion av narkotika och sprängämnen på flygplatser.

En biosensor består av biologiska molekyler som reagerar med analyten samt ett givarelement (transducer) som kan detektera och omvandla den biomolekylära reaktionen till en observerbar signal.

Den biomolekylära reaktionen kan basera sig på flera olika principer och typer av molekyler. När det gäller specifik detektering av olika molekyler, har den så kallade immunosensorn, som använder sig av samma typ av molekyler och inbindningar som kroppens egna immunförsvar, kommit att få en stor betydelse. Man använder sig då av antikroppar specifikt framtagna för den aktuella analyten.

Det har blivit mer och mer vanligt att använda sig av så kallad markörsfria (label-free) immunosensorer, där man oftast använder sig av optiska eller akustiska givare för att direkt mäta en inbindning till en yta utan att fluorescerande eller radioaktiva markörer krävs. Då det gäller den akustiska metoden kan man använda sig av så kallade piezoelektriska material som direkt kan excitera och detektera akustiska vågor elektriskt. Komponenter som använder sig av piezoelektriska material brukar kallas elektroakustiska.

Denna avhandling har fokuserat på en ny typ av elektroakustisk komponent och dess potential som ett givarelement (transducer) för biosensor tillämpningar. Den är tillverkad med hjälp av tunnfilmsteknik, som är samma typ av masstillverkningsteknik som används i elektronikindustrin. Det gör den mycket lämplig för integrering med den omgivande elektroniken.

Komponenten är en så kallad tunnfilmbaserad bulkakustisk resonator FBAR (Thin Film Bulk Acoustic Resonator) som började användas för några år sedan inom telekomindustrin för tillverkning av högfrekvensfilter för mobiltelefoner. De har varit i kommersiella produkter sedan 2001.

Biosensorer måste fungera i vätska för att biomolekylerna inte ska förstöras. I dess konventionella form fungerar FBAR därför inte som biosensor, då den akustiska våg den använder inte lämpar sig för vätska. Förlusterna skulle bli för stora.

Inom ramen för denna avhandling har det därför tagits fram en ny metod för att växa det piezoelektriska materialet (aluminiumnitrid) på ett sådant sätt så att det möjliggör excitering av en annan akustisk våg som lämpar sig för vätskebaserade miljöer och därmed biosensorer.

Med hjälp av denna nya teknik kan man tillverka en ny typ av FBAR, som fungerar enligt samma princip som en speciell typ av kvartskristallkomponent, som har använts som biosensor de senaste 20 åren. Den kallas QCM (Quartz Crystal Microbalance) och består av en skiva kvarts som vibrerar genom skjuvning av kristallen. Den mekaniska resonansfrekvensen kan genom den piezoelektriska effekten i kristallen

exciteras och detekteras elektriskt. Resonansfrekvensen är känslig mot ändringar i akustiska egenskaper i det mediumet som är i kontakt med kristallytan. En biomolekylär inbindning på ytan kan därmed detekteras som en ändring i resonansfrekvensen. Resonansfrekvensen för QCM ligger oftast på 5-20MHz. Den nya typen av FBAR fungerar enligt samma princip som QCM men resonansfrekvensen är mycket högre – kring 1GHz. FBAR är till skillnad från QCM tillverkat med metoder som lämpar sig för integrering med elektroniken.

Den extremt höga frekvensen gör att FBAR kommer att fungera något annorlunda än QCM. I denna avhandling har det studerats hur denna mycket höga frekvens kommer att påverka känsligheten, brusnivån och dämpningen i vätska. Allt detta kommer att bestämma upplösningen man kan uppnå med sensorn. I avhandlingen visas att den förväntade upplösningen är redan nu på samma nivå och kanske något bättre som den konventionella QCMen. Vidare demonstreras en temperaturstabil FBAR som ytterligare förbättrar stabiliteten. En komplett immunosensor presenteras också för detektering av narkotika. Mycket arbete har dedikerats till att förstå hur FBAREns olika delar inverkar på prestandan. Simuleringar har gjorts för att studera hur den akustiska vågen propagerar i FBAREns olika lager och ut i den omgivande vätskan.

Resultaten visar på en stor potential för den nya typen av FBAR som en biosensor. Vilket möjliggör masstillverkning av miniaturiserade biosensorer och biosensor arrayer som är integrerade med elektroniken.

References

- [1] P. D. Skottrup, M. Nicolaisen, and A. F. Justesen, "Towards on-site pathogen detection using antibody-based sensors," *Biosensors and Bioelectronics*, vol. 24, pp. 339-348, 2008.
- [2] K. A. Marx, "Quartz crystal microbalance: A useful tool for studying thin polymer films and complex biomolecular systems at the solution - Surface interface," *Biomacromolecules*, vol. 4, pp. 1099-1120, 2003.
- [3] J. F. Rosenbaum, *Bulk Acoustic Wave Theory and Devices*: Artech House, 1988.
- [4] H. Nowotny and E. Benes, "General one-dimensional treatment of the layered piezoelectric resonator with two electrodes," *Journal of the Acoustical Society of America*, vol. 82, pp. 513-21, 1987/08/1987.
- [5] B. R. Eggins, *Chemical sensors and biosensors*: John Wiley & Sons Ltd., 2002.
- [6] D. S. Ballantine, R. M. White, S. J. Martin, A. J. Ricco, E. T. Zellers, G. C. Frye, and H. Wohltjen, *Acoustic wave sensors; theory, design, and physico - chemical applications*: Academic Press, 1997.
- [7] W. G. Cady, "New methods for maintaining constant frequency in high-frequency circuits," *Physical Review*, vol. 18, pp. 142-143, 1921.
- [8] F. R. Lack, G. W. Willard, and I. E. Fair, "Quartz crystal circuit elements," *Bell System Technical Journal*, vol. 13, pp. 453-463, 1934.
- [9] M. Baker and Laurenso.L, "Use of a Quartz Crystal Microbalance for Measuring Vapour Backstreaming from Mechanical Pumps," *Vacuum*, vol. 16, pp. 633-&, 1966.
- [10] W. H. King and L. W. Corbett, "Relative Oxygen Absorption and Volatility Properties of Sub-Micron Films of Asphalt Using Quartz Crystal Microbalance," *Abstracts of Papers of the American Chemical Society*, pp. PE21-&, 1969.
- [11] L. L. Levenson, "Sticking Coefficient Measurements at Cryogenic Temperatures with a Resonating Quartz Crystal Microbalance," *Vacuum*, vol. 15, pp. 255-&, 1965.

- [12] M. Shiojiri, Y. Hasegawa, Y. Murata, and Matsumur.S, "Quartz Crystal Microbalance Techniques Applicable to Studies of Sulphuration and Oxidation of Thin Metal Films," *Japanese Journal of Applied Physics*, vol. 8, pp. 783-&, 1969.
- [13] W. H. King, Jr., "Piezoelectric sorption detector," *Analytical Chemistry*, vol. 36, pp. 1735-1738, 1964.
- [14] T. Nomura and M. Okuhara, "Frequency-Shifts of Piezoelectric Quartz Crystals Immersed in Organic Liquids," *Analytica Chimica Acta*, vol. 142, pp. 281-284, 1982.
- [15] S. Kurosawa, E. Tawara, N. Kamo, and Y. Kobatake, "Oscillating Frequency of Piezoelectric Quartz Crystal in Solutions," *Analytica Chimica Acta*, vol. 230, pp. 41-49, Mar 1990.
- [16] K. K. Kanazawa and J. G. Gordon, "Frequency of a quartz microbalance in contact with liquid," *Anal. Chem.*, vol. 57, pp. 1770-1771, 1985.
- [17] C. D. Stockbridge, "Effects of gas pressure on quartz-crystal microbalances," 1966, pp. 147-178.
- [18] M. Rodahl, F. Hook, A. Krozer, P. Brzezinski, and B. Kasemo, "Quartz crystal microbalance setup for frequency and Q-factor measurements in gaseous and liquid environments," *Review of Scientific Instruments*, vol. 66, p. 3924, 1995.
- [19] M. V. Voinova, M. Rodahl, M. Jonson, and B. Kasemo, "Viscoelastic acoustic response of layered polymer films at fluid-solid interfaces: continuum mechanics approach," *Physica Scripta*, vol. 59, pp. 391-6, 1999.
- [20] G. Sauerbrey, "Use of quartz vibrator for weighing thin layers and as a micro-balance," *Zeitschrift fur Physik*, vol. 155, pp. 206-222, 1959.
- [21] R. Lucklum and P. Hauptmann, "Acoustic microsensors-the challenge behind microgravimetry," *Analytical and Bioanalytical Chemistry*, vol. 384, pp. 667-682, 2006.
- [22] M. Thompson, A. L. Kipling, W. C. Duncanhewitt, L. V. Rajakovic, and B. A. Cavicvlasak, "Thickness-Shear-Mode Acoustic-Wave Sensors in the Liquid-Phase - a Review," *Analyst*, vol. 116, pp. 881-890, Sep 1991.
- [23] N. J. Cho, J. N. D'Amour, J. Stalgren, W. Knoll, K. Kanazawa, and C. W. Frank, "Quartz resonator signatures under Newtonian liquid loading for initial instrument check," *Journal of Colloid and Interface Science*, vol. 315, pp. 248-254, Nov 2007.
- [24] L. Daikhin and M. Urbakh, "Influence of surface roughness on the quartz crystal microbalance response in a solution: new configuration for QCM studies," UK, 1997, pp. 27-38.
- [25] L. Macakova, E. Blomberg, and P. M. Claesson, "Effect of adsorbed layer surface roughness on the QCM-D response: Focus on trapped water," *Langmuir*, vol. 23, pp. 12436-12444, 2007.
- [26] S. J. Martin, G. C. Frye, A. J. Ricco, and S. D. Senturia, "Effect of surface roughness on the response of thickness-shear mode resonators in liquids," *Anal. Chem.*, vol. 65, pp. 2910-2922, 1993.

- [27] L. Rodriguez-Pardo, J. F. Rodriguez, C. Gabrielli, H. Perrot, and R. Brendel, "Sensitivity, noise, and Resolution in QCM sensors in liquid media," *IEEE Sensors Journal*, vol. 5, pp. 1251-1256, 2005.
- [28] F. Lu, H. P. Lee, and S. P. Lim, "Mechanical description of interfacial slips for quartz crystal microbalances with viscoelastic liquid loading," *Smart Materials and Structures*, vol. 12, pp. 881-888, 2003.
- [29] S. J. Martin and G. C. Frye, "Polymer film characterization using quartz resonators," *IEEE 1991 Ultrasonics Symposium Proceedings*, pp. 393-8, 1991.
- [30] R. Lucklum and P. Hauptmann, "Quartz crystal microbalance: mass sensitivity, viscoelasticity and acoustic amplification," *Sensors and Actuators, B: Chemical*, vol. 70, pp. 30-36, 2000.
- [31] F. Höök and B. Kasemo, "The QCM-D Technique for Probing Biomacromolecular Recognition Reactions " in *Piezoelectric Sensors*. vol. C: Springer Berlin Heidelberg, 2006, pp. 425-447.
- [32] C. Larsson, M. Rodahl, and F. Hook, "Characterization of DNA immobilization and subsequent hybridization on a 2D arrangement of streptavidin on a biotin-modified lipid bilayer supported on SiO₂," *Analytical Chemistry*, vol. 75, pp. 5080-5087, Oct 2003.
- [33] M. P. Jonsson, P. Jonsson, and F. Hook, "Simultaneous nanoplasmonic and quartz crystal microbalance sensing: Analysis of biomolecular conformational changes and quantification of the bound molecular mass," *Analytical Chemistry*, vol. 80, pp. 7988-7995, 2008.
- [34] E. Reimhult, C. Larsson, B. Kasemo, and F. Hook, "Simultaneous surface plasmon resonance and quartz crystal microbalance with dissipation monitoring measurements of biomolecular adsorption events involving structural transformations and variations in coupled water," *Analytical Chemistry*, vol. 76, pp. 7211-7220, 2004.
- [35] M. Edvardsson, S. Svedhem, G. Wang, R. Richter, M. Rodahl, and B. Kasemo, "QCM-D and Reflectometry Instrument: Applications to Supported Lipid Structures and Their Biomolecular Interactions," *Analytical Chemistry*, vol. 81, pp. 349-361, Jan 2009.
- [36] G. Wang, M. Rodahl, M. Edvardsson, S. Svedhem, G. Ohlsson, F. Hook, and B. Kasemo, "A combined reflectometry and quartz crystal microbalance with dissipation setup for surface interaction studies," *Review of Scientific Instruments*, vol. 79, pp. 075107-1, 2008.
- [37] T. W. Grudkowski, J. F. Black, T. M. Reeder, D. E. Cullen, and R. A. Wagner, "Fundamental-Mode Vhf-Uhf Miniature Acoustic Resonators and Filters on Silicon," *Applied Physics Letters*, vol. 37, pp. 993-995, 1980.
- [38] K. M. Lakin and J. S. Wang, "Acoustic Bulk Wave Composite Resonators," *Applied Physics Letters*, vol. 38, pp. 125-127, 1981.
- [39] K. M. Lakin, J. S. Wang, G. R. Kline, A. R. Landin, Y. Y. Chen, and J. D. Hunt, "THIN FILM RESONATORS AND FILTERS," *Ultrasonics Symposium Proceedings*, vol. 1, pp. 466-475, 1982.

- [40] M. T. Wauk and D. K. Winslow, "Vacuum deposition of AlN acoustic transducers," *Applied Physics Letters*, vol. 13, pp. 286-288, 1968.
- [41] R. M. Malbon, D. J. Walsh, and D. K. Winslow, "Zinc-oxide film microwave acoustic transducers," *Applied Physics Letters*, vol. 10, pp. 9-10, 1967.
- [42] H. M. Manasevit, F. M. Erdmann, and W. I. Simpson, "The use of metalorganics in the preparation of semiconductor materials. IV. The nitrides of aluminum and gallium," *Journal of the Electrochemical Society*, vol. 118, pp. 1864-8, 1971.
- [43] M. T. Duffy, C. C. Wang, G. D. O'Clock, Jr., S. H. McFarlane, III, and P. J. Zanzucchi, "Epitaxial growth and piezoelectric properties of AlN, GaN, and GaAs on sapphire or spinel," *Journal of Electronic Materials*, vol. 2, pp. 359-72, 1973.
- [44] G. A. Rozgonyi and W. J. Polito, "Preparation of ZnO thin films by sputtering of the compound in oxygen and argon," *Applied Physics Letters*, vol. 8, pp. 220-221, 1966.
- [45] A. J. Noreika, M. H. Francombe, and S. A. Zeitman, "DIELECTRIC PROPERTIES OF REACTIVELY SPUTTERED FILMS OF ALUMINUM NITRIDE," vol. 6, pp. 194-7, 1969.
- [46] R. F. Rutz, E. P. Harris, and J. J. Cuomo, "An AlN switchable memory resistor capable of a 20-MHz cycling rate and 500-picosecond switching time," *IBM Journal of Research and Development*, vol. 17, pp. 61-5, 1973.
- [47] G. A. Rozgonyi and W. J. Polito, "Epitaxial thin films of ZnO on CdS and sapphire," *Journal of Vacuum Science and Technology*, vol. 6, pp. 115-119, 1969.
- [48] A. J. Shuskus, T. M. Reeder, and E. L. Paradis, "RF-sputtered aluminium nitride films on sapphire," *Applied Physics Letters*, vol. 24, pp. 155-6, 1974.
- [49] S. Yoshida, S. Misawa, Y. Fujii, S. Takada, H. Hayakawa, S. Gonda, and A. Itoh, "Reactive molecular beam epitaxy of aluminium nitride," *Journal of Vacuum Science and Technology*, vol. 16, pp. 990-3, 1979.
- [50] T. Shiosaki, T. Yamamoto, T. Oda, and A. Kawabata, "Low-temperature growth of piezoelectric AlN film by RF reactive planar magnetron sputtering," *Applied Physics Letters*, vol. 36, pp. 643-5, 1980.
- [51] J. S. Wang and K. M. Lakin, "Low-temperature coefficient bulk acoustic wave composite resonators," *Applied Physics Letters*, vol. 40, pp. 308-10, 1982.
- [52] J. S. Wang, A. Kong, K. F. Lau, and K. H. Yen, "Recent developments on membrane bulk-acoustic-wave resonators," *Proceedings IEEE Frequency Control Symposium*, pp. 356-60, 1985.
- [53] G. R. Kline and K. M. Lakin, "1.0-GHz thin-film bulk acoustic wave resonators on GaAs," *Applied Physics Letters*, vol. 43, pp. 750-1, 1983.

- [54] M. M. Driscoll, R. A. Moor, J. F. Rosenbaum, S. V. Krishnaswamy, and J. R. Szedon, "Recent advances in monolithic film resonator technology," New York, NY, USA, 1986, pp. 365-9.
- [55] K. M. Lakin, K. T. McCarron, and R. E. Rose, "Solidly mounted resonators and filters," in *1995 IEEE Ultrasonics Symposium*, Seattle, Wa, 1995, pp. 905-908.
- [56] H. Lakdawala and E. S. Kim, "Simple post-processing technique to tune resonant frequency of film bulk acoustic resonators and stacked crystal filters," in *IEEE International Frequency Control Symposium*, Pasadena, Ca, 1998, pp. 831-835.
- [57] R. Ruby, "Review and comparison of bulk acoustic wave FBAR, SMR technology," in *IEEE Ultrasonics Symposium*, New York, NY, 2007, pp. 1029-1040.
- [58] J. D. Larson, III, R. Ruby, P. Bradley, and Y. Oshmyansky, "A BAW antenna duplexer for the 1900 MHz PCS band," Piscataway, NJ, USA, 1999, pp. 887-90.
- [59] R. C. Ruby, P. Bradley, Y. Oshmyansky, A. Chien, and J. D. Larson III, "Thin film bulk wave acoustic resonators (FBAR) for wireless applications," 2001, pp. 813-821.
- [60] J. D. Larson, III, P. D. Bradley, S. Wartenberg, and R. C. Ruby, "Modified Butterworth-Van Dyke circuit for FBAR resonators and automated measurement system," Piscataway, NJ, USA, 2000, pp. 863-8.
- [61] K. Wang, W. Mueller, R. Ruby, M. Gat, P. Bradley, A. Barfknecht, F. Geefay, C. Han, G. Gan, A. Chien, and B. Ly, "High rejection Rx filters for GSM handsets with wafer level packaging," 2002, pp. 925-929.
- [62] R. Aigner, "SAW and BAW Technologies for RF Filter Applications: A review of the Relative Strengths and Weaknesses," in *IEEE Ultrasonics Symposium*, Beijing, China, 2008.
- [63] V. Yantchev and I. Katardjiev, "Thin AlN film resonators utilizing the lowest order symmetric Lamb mode: Further developments," *IEEE International Frequency Control Symposium*, pp. 1067-1072, 2007.
- [64] J. H. Kuypers, L. Chih-Ming, G. Vigevani, and A. P. Pisano, "Intrinsic temperature compensation of aluminum nitride Lamb wave resonators for multiple-frequency references," *2008 IEEE International Frequency Control Symposium*, pp. 240-9, 2008.
- [65] K. M. Lakin, J. Belsick, J. F. McDonald, and K. T. McCarron, "Improved bulk wave resonator coupling coefficient for wide bandwidth filters," *IEEE Ultrasonics Symposium Proceedings*, vol. vol.1, pp. 827-31, 2001.
- [66] R. Thalhammer, J. Kaitila, S. Zieglmeier, and L. Elbrecht, "Spurious mode suppression in BAW resonators," in *IEEE Ultrasonics Symposium*, Vancouver, CANADA, 2006, pp. 456-459.
- [67] D. McNamara, "FBAR technology shrinks CDMA handset duplexers," *Microwaves & RF*, vol. 39, pp. 71-9, 2000.

- [68] R. C. Ruby, P. Bradley, Y. Oshmyansky, A. Chien, and J. D. Larson Iii, "Thin film bulk wave acoustic resonators (FBAR) for wireless applications," *IEEE Ultrasonics Symposium Proceedings*, vol. 1, pp. 813-821, 2001.
- [69] M. Minakata, N. Chubachi, and Y. Kikuchi, "Variation of c-axis orientation of ZnO thin films deposited by DC diode sputtering," *Japanese Journal of Applied Physics*, vol. 12, pp. 474-5, 1973.
- [70] J. S. Wang and K. M. Lakin, "Sputtered C-axis inclined ZnO films for shear wave resonators," *Ultrasonics Symposium Proceedings*, pp. 480-3, 1982.
- [71] J. S. Wang, K. M. Lakin, and A. R. Landin, "Sputtered C-Axis Inclined Piezoelectric Films and Shear-Wave Resonators," *Ieee Transactions on Sonics and Ultrasonics*, vol. 30, pp. 391-392, 1983.
- [72] N. F. Foster, "Performance of shear mode zinc oxide thin-film ultrasonic transducers," *Journal of Applied Physics*, vol. 40, pp. 4202-4, 1969.
- [73] M. Link, M. Schreiter, J. Weber, D. Pitzer, R. Primig, M. B. As-souar, and O. Elmazria, "C-axis inclined ZnO films deposited by reactive sputtering using an additional blind for shear BAW devices," *IEEE International Ultrasonics Symposium*, pp. 202-205, Sep 18-21 2005.
- [74] J. Weber, W. M. Albers, J. Tuppurainen, M. Link, R. Gabl, W. Wersing, and M. Schreiter, "Shear mode FBARs as highly sensitive liquid biosensors," *Sensors and Actuators a-Physical*, vol. 128, pp. 84-88, Mar 2006.
- [75] T. Yanagitani, M. Kiuchi, M. Matsukawa, and Y. Watanabe, "Characteristics of pure-shear mode BAW resonators consisting of (11 $\bar{2}$ 0) textured ZnO films," *Ieee Transactions on Ultrasonics Ferroelectrics and Frequency Control*, vol. 54, pp. 1680-1686, Aug 2007.
- [76] T. Matsuo, T. Yanagitani, M. Matsukawa, and Y. Watanabe, "Highly oriented c-axis 23 degrees tilted ZnO films with high quasi-shear mode electromechanical coupling coefficients," in *IEEE Ultrasonics Symposium*, New York, NY, 2007, pp. 1229-1232.
- [77] T. Yanagitani and M. Muchi, "Highly oriented ZnO thin films deposited by grazing ion-beam sputtering: Application to acoustic shear wave excitation in the GHz range," *Japanese Journal of Applied Physics Part 2-Letters & Express Letters*, vol. 46, pp. L1167-L1169, Dec 2007.
- [78] E. Milyutin, S. Gentil, and P. Muralt, "Shear mode bulk acoustic wave resonator based on c-axis oriented AlN thin film," *Journal of Applied Physics*, vol. 104, p. 6, Oct 2008.
- [79] E. Milyutin and P. Muralt, "Shear mode BAW resonator based on c-axis oriented AlN thin film," in *IEEE Ultrasonics Symposium Beijing, China*, 2008.

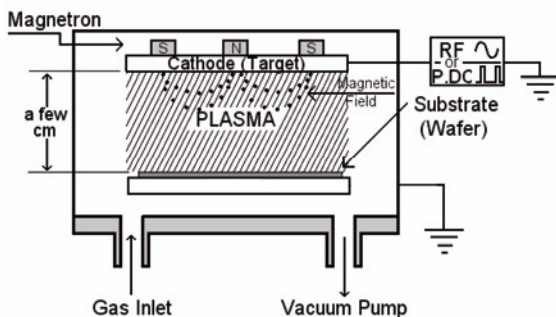
- [80] J. Bjurström, D. Rosen, I. Katardjiev, V. M. Yanchev, and I. Petrov, "Dependence of the electromechanical coupling on the degree of orientation of c-textured thin AlN films," *Ieee Transactions on Ultrasonics Ferroelectrics and Frequency Control*, vol. 51, pp. 1347-1353, Oct 2004.
- [81] J. Bjurström, "Advanced Thin Film Electroacoustic devices," Ph. Doctoral Thesis, Uppsala University, 2007.
- [82] I. Katardjiev, J. Bjurström, and G. Wingqvist, "Production of polycrystalline films for shear mode piezoelectric thin film resonators ", International patent application PCT/SE2006/050041, 2006 ed Sweden, 2006.
- [83] F. Engelman, "AlN and high-*k* thin films for IC and electroacoustic applications," Ph. Doctoral Thesis, Uppsala University, 2002, p. 80.
- [84] M. Rodahl, F. Hook, and B. Kasemo, "QCM operation in liquids: An explanation of measured variations in frequency and Q factor with liquid conductivity," *Analytical Chemistry*, vol. 68, pp. 2219-2227, Jul 1996.
- [85] G. Sharma, J. Enlund, J. Bjurström, L. Liljeholm, I. Katardjiev, and K. Hjort, "Fabrication and characterization of a shear mode AlN solidly mounted resonator-silicone microfluidic system for in-liquid sensor applications," *Sensors & Actuators: A*, submitted to.
- [86] J. S. Wang, A. R. Landin, and M. M. Lakin, "Low temperature coefficient shear wave thin films for composite resonators and filters," *Proceedings IEEE Ultrasonics Symposium* pp. 491-4, 1983.
- [87] J. R. Vig, "On Acoustic Sensor Sensitivity," *Ieee Transactions on Ultrasonics Ferroelectrics and Frequency Control*, vol. 38, pp. 311-311, May 1991.
- [88] J. R. Vig and F. L. Walls, "A review of sensor sensitivity and stability," *IEEE/EIA International Frequency Control Symposium and Exhibition Proceedings*, pp. 30-33, 2000.
- [89] "IEEE standard on piezoelectricity," Inst. Electr. & Electron. Eng., New York, NY, USA, Copyright 1988, IEE ANSI/IEEE Std 176-1987, 1988.
- [90] "IEEE standard definitions of physical quantities for fundamental frequency and time metrology - random instabilities," *IEEE Std 1139-1999*, 1999.
- [91] J. Weber, W. M. Albers, J. Tuppurainen, M. Link, R. Gabl, W. Wersing, and M. Schreiter, "Shear mode FBARs as highly sensitive liquid biosensors," *Sensors and Actuators A: Physical*, vol. 128, pp. 84-88, 2006.
- [92] J. D. Larson, R. Ruby, and P. Bradley, "Bulk acoustic wave resonator with improved lateral mode suppression," *U.S. Patent 6215375*, 2001.
- [93] D. Rosen, J. Bjurström, and I. Katardjiev, "Suppression of spurious lateral modes in thickness-excited FBAR resonators," *Ieee Transactions on Ultrasonics Ferroelectrics and Frequency Control*, vol. 52, pp. 1189-1192, Jul 2005.

- [94] J. Kaitila, M. Ylilammi, J. Ella, and R. Aigner, "Spurious resonance free bulk acoustic wave resonators," in *IEEE International Ultrasonics Symposium*, Honolulu, HI, 2003, pp. 84-87.
- [95] S. Marksteiner, J. Kaitila, G. G. Fattinger, and R. Aigner, "Optimization of acoustic mirrors for solidly mounted BAW resonators," in *IEEE International Ultrasonics Symposium*, Rotterdam, NETHERLANDS, 2005, pp. 329-332.
- [96] A. Alippi, F. Craciun, and E. Molinari, "Piezoelectric plate resonances due to first Lamb symmetrical mode," *Journal of Applied Physics*, vol. 64, pp. 2238-40, 1988.
- [97] M. Desvergne, E. Defay, D. Wolozan, M. Aid, P. Vincent, A. Volatier, Y. Deval, and J. B. Begueret, "Intermediate frequency lamb wave coupled resonator filters for RF receiver architectures," *Proceedings of the 37th European Solid-State Device Research Conference*, pp. 358-61, 2007.
- [98] P. J. Stephanou and A. P. Pisano, "GHz contour extensional mode aluminum nitride MEMS resonators," *IEEE Ultrasonics Symposium*, p. 4 pp., 2006.
- [99] Y. Nakagawa, S. Tanaka, and S. Kakio, "Lamb-wave-type high frequency resonator," *Japanese Journal of Applied Physics, Part 1: Regular Papers and Short Notes and Review Papers*, vol. 42, pp. 3086-3090, 2003.
- [100] V. Yantchev and I. Katardjiev, "Micromachined thin film plate acoustic resonators utilizing the lowest order symmetric lamb wave mode," *IEEE Transactions on Ultrasonics, Ferroelectrics and Frequency Control*, vol. 54, pp. 87-95, 2007.
- [101] D. M. Martin, V. Yantchev, and I. Katardjiev, "Buried electrode electroacoustic technology for the fabrication of thin film based resonant components," *Journal of Micromechanics and Microengineering*, vol. 16, pp. 1869-74, 2006.
- [102] J. Bjurstrom, V. Yantchev, and I. Katardjiev, "Thin film Lamb wave resonant structures - The first approach," *Solid-State Electronics*, vol. 50, pp. 322-326, Mar 2006.
- [103] V. Yantchev, J. Enlund, J. Biurstrom, and I. Katardjiev, "Design of high frequency piezoelectric resonators utilizing laterally propagating fast modes in thin aluminum nitride (AlN) films," *Ultrasonics*, vol. 45, pp. 208-212, Dec 2006.
- [104] W. Pang, R. C. Ruby, R. Parker, P. W. Fisher, J. D. Larson Iii, K. J. Grannen, D. Lee, C. Feng, and L. Callaghan, "A thermally stable CMOS oscillator using temperature compensated FBAR," *IEEE Ultrasonics Symposium*, pp. 1041-1044, 2007.
- [105] C. S. Lam, C. Y. J. Wang, and S. M. Wang, "A Review of the Recent Development of Temperature Stable Cuts of Quartz for SAW Applications," in *Symposium on Piezoelectricity, Acoustic Waves, and Device Applications*, 2008.

Appendix A Sputtering

Sputter deposition is a physical vapor deposition (PVD) process where atoms in a solid target material are ejected (sputtered) into gas phase due to bombardment of the material by energetic ions. The sputtered atoms are not in thermodynamic equilibrium with the surrounding gas as they initially possess relatively high kinetic energies equal on average half the sublimation energy of the target material. At standard operating pressures and target to substrate distances the sputtered atoms normally experience a number of gas phase collisions until they finally deposit (condense into solid matter) on all surfaces in the vacuum chamber. A substrate (such as a Si-wafer) placed in the chamber will be coated with a thin film.

The high-energy ions used in sputter-deposition are generated by glow discharges. A glow discharge is a self-sustained type of plasma created by applying an electrical field to a pressurized gas, creating free electrons within the discharge region. Sputtering usually uses argon plasma, due to the non-reactive behavior of argon. A gas combination containing partial pressure of reactive gases could also be used to create oxides or nitrides through chemical reactions with the target species; this is then called *reactive sputtering*.



Sputtering as a deposition technique may be described as a sequence of these steps:

- 1) ions are generated and directed at a target material
- 2) the ions sputter atoms from the target
- 3) the sputtered atoms get transported to the substrate through a region of reduced pressure
- 4) the sputtered atoms condense on the substrate, forming a thin film.

A set of permanent magnets is normally installed *on the back side of* the target to increase the efficiency of sputtering by providing a closed magnetic field parallel to the target surface – a configuration normally referred to as magnetron. Thus, secondary electrons ejected from the cathode (target) and accelerated by the electric field are trapped by the magnetic field increasing in this way their ionization efficiency. The latter leads to an increased plasma density and hence to an increased erosion rate. This is most pronounced at areas on the target where the magnetic field is strongest and typically represents a pronounced erosion track in the form of a circle, normally called the *race track*.

Reactive sputtering

By introducing a reactive gas into the chamber chemical reactions will take place between the gas molecules as well as eventual radicals on the one hand and the sputtered species condensed on chamber surfaces including substrate surface on the other. In addition, chemical reactions may also take place at the target surface, a process normally referred to as target poisoning. At low partial pressures of the reactive gas and high enough sputtering rates, the gettering rate of all chamber surfaces is sufficient to keep the target only marginally covered with a compound and the sputtering behavior is close to the one of pure metal target. To obtain films with correct stoichiometry it is often required to increase the reactive partial pressure. As the latter increases a compound layer, typically a dielectric, gradually grows onto the target which in turn alters its electrical behavior. Thus, as the target surface is continually bombarded by positive ions these charge up the compound layer resulting in a voltage drop across the latter. This voltage drop gradually increases decreasing effectively the potential difference between the target surface and the plasma until finally the discharge is extinguished. Intermittent effect such as electrical breakdown discharges at specific spots on the target surface due to local inhomogeneities in the compound layer cause arcing and subsequent release of material in the form of macroparticles or flakes. In order to avoid charging and flaking short positive pulses are applied to the target to the effect of discharging the compound layer. Such discharges are called pulsed DC sputtering.

Historically, RF discharges have been employed for reactive sputter deposition or for the sputtering of insulating targets. Pulsed DC sputtering, however, provides higher deposition rates.

Von Ardenne Sputtering system - Uppsala University

The sputtering system, inhere used, is a conventional sputtering system Von Ardenne-CS 730 (Von Ardenne Anlagentechnik GmbH, Dresden, Germany). The system is a 2-chamber system with a common load lock and transfer chamber. There are 4 target positions in each chamber. The circular wafer holder table can contain 4 wafers and can automatically be rotated to

deposit each wafer separately in a sequence. The substrate is placed parallel and right underneath the target. The distance is about 5.5cm. In between the target and the substrate there is a shutter shield, which can be rotated into 4 positions. No modifications to the system have been made.

The AlN was deposited using a 15cm diameter, 99.999% pure Al target with a balanced magnetron. Base pressure was usually well below $5 \cdot 10^{-8}$ Torr. The gas mixture was Ar:N₂ varied from 8:52 to 24:36 in flow ratios keeping the total flow constant at 60sccm¹⁷. Pulsed DC was applied and the discharge power was 900-1200W. The substrate holder plate was at floating potential and no heating was applied.

¹⁷ sccm = Standard Cubic Centimeters per Minute

Appendix B

AlN

In section 2.1 an introduction is given to AlN. Further summaries on the properties of AlN can be found in for example prior doctoral thesis [81].

Here a summary is given on the major planes in the hexagonal AlN structure and the angle their normal form with the c-axis. This is of interest when studying the influence of the seed layer in the 2-step deposition process described in section 2.2.

set of planes	2θ	c-axis inclination
{100}	33.226	90°
{002}	36.056	0°
{101}	37.943	58°
{102}	49.838	38°
{110}	59.367	90°
{103}	66.077	28°
{112}	71.460	48°




Some major sets of crystal planes in the AlN hexagonal structure. They are presented along with there X-ray diffraction angle (2θ). The “c-axis inclination” refers to the angle between the plane normal and the c-axis of the AlN hexagonal primitive unit cell structure.

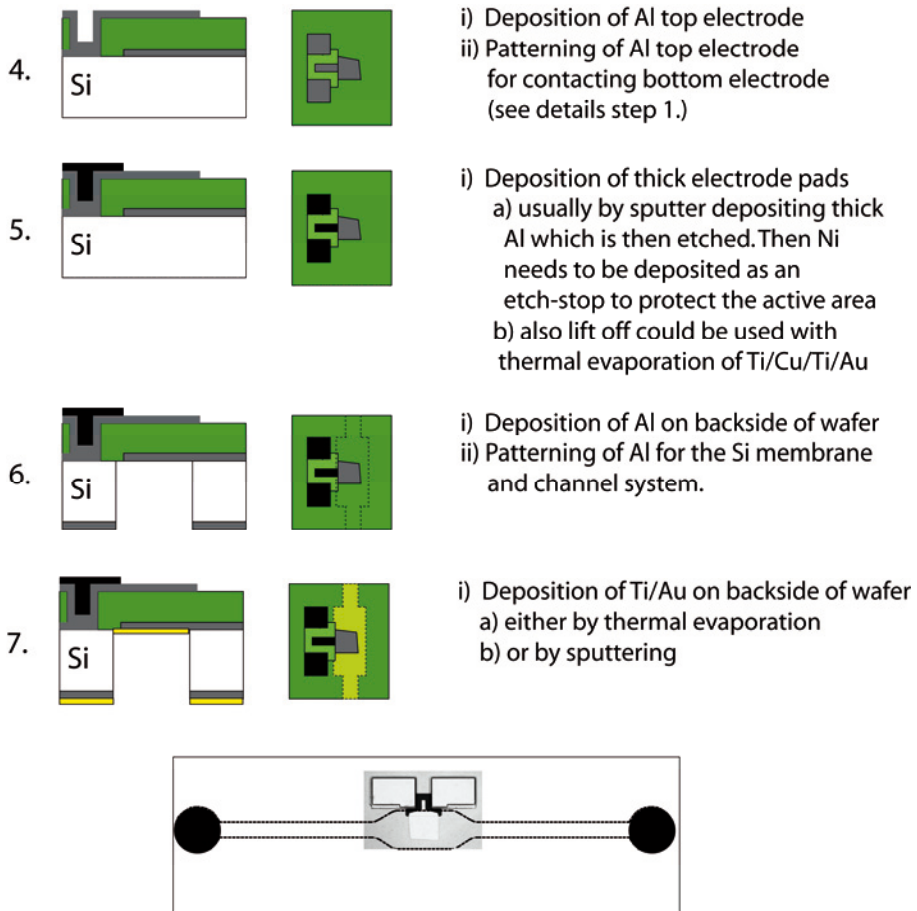
Appendix C

Fabrication of a typical FBAR sensor

sensor

■ Al ■ Ni ■ AlN ■ Thick electrode

1. 
 - i) Deposition of Al bottom electrode
 - ii) Patterning of bottom electrode to avoid parasitic capacitances
 - a) either by wet etching using commercial chemicals
 - b) or by dry reactive ion etching using $(\text{Cl}_2/\text{BCl}_3/\text{O}_2/\text{Ar})$ -plasma
2. 
 - i) Deposition of Ni etch stop
 - ii) Patterning of Ni etch stop (usually this is done with lift-off)
3. 
 - i) Deposition of AlN
 - ii) Patterning of AlN to create via-holes for contacting bottom electrode and create openings for the sample injection
 - reactive ion etching with $(\text{Cl}_2/\text{BCl}_3/\text{O}_2/\text{Ar})$ -plasma is used:
 - a) either a hard mask of Ni (pattern with Al mask) is used
 - b) or a thick photoresist mask.
 - iii) The Ni mask and etch stop is etched in HNO_3



Note that this is a schematic flow chart representing the main fabrication steps of the FBAR sensors used inhere. It does not show every variation utilized or every suggested optimization (see section 3).

It is further noted that a number of optimization and control measurements is included in the necessary steps for FBAR fabrication especially concerning the reactive sputtering process of AlN. Such optimization and control measurements would typically involve XRD measurements of the crystalline structure in addition to thickness and stress measurements.

Appendix D

Simulation models and implementation of the Mason model

The electrical interpretation of the Mason model has been well described in text books [3]. Therefore, only a brief description will be given here along with the implementation used within this thesis.

The Mason model is based on the transmission line model. A *transmission line* is a material medium or structure that forms all or part of a path for transmission of energy by wave motion from one point to another. By wave motion it is meant electromagnetic wave or acoustic wave propagation as well as electric power transmission. Components of transmission lines include wires, coaxial cables, dielectric slabs, optical fibers, electric power lines, and waveguides.

It could be stated an analogy between the electromagnetic and the acoustic transmission line where the electrical voltage is the acoustic *force* (F) and the electrical current is the acoustic *displacement velocity* (v). The ratio between the force and the velocity at a boundary is called the *input acoustic impedance*.

Each layer in the acoustic structure is assumed to be homogeneous. The acoustic waves are assumed to be propagating plane waves (in the z direction). At each border there will be a reflection due impedance mismatch. Therefore, the displacement amplitude distribution inside a given layer could be written as a superposition of plane waves traveling in the forward and backward directions:

$$u = (a \cdot e^{-ikz} + b \cdot e^{ikz})e^{i\omega t} \quad ^{18} \quad (1)$$

¹⁸ ω is the angular frequency. k is the wave number.

The displacement velocity is then $v=i\omega u$. v_n and v_{n+1} are the velocities at the boundaries of the layer respectively. The thickness of the layer is d . The a and b coefficients can then be extracted as:

$$\begin{aligned} a &= \frac{v_n e^{ikz} - v_{n+1} e^{ikz}}{-2\omega \sin(kd)} \\ b &= \frac{v_{n+1} e^{-ikz} - v_n e^{-ikz}}{-2\omega \sin(kd)} \end{aligned} \quad (2)$$

Non-piezoelectrically active layers

In a purely acoustic layer the mechanical force (F) is:

$$F = A \cdot X = A \cdot c \cdot S = A \cdot c \cdot \frac{\partial u}{\partial z} = ikcA(-a \cdot e^{-ikz} + b \cdot e^{ikz})e^{i\omega t} \quad 19$$

By applying these sets of equations at the boundaries the relation between the velocity and force at the two boundaries could be described in a matrix form as:

$$\begin{pmatrix} v_n \\ F_n \end{pmatrix} = T_n \begin{pmatrix} v_{n+1} \\ F_{n+1} \end{pmatrix}, \quad (3)$$

where T is a 2-by-2 transformation matrix. In the multiple layer case it will then be:

$$\begin{pmatrix} v_0 \\ F_0 \end{pmatrix} = T_0 T_1 \cdots T_m \begin{pmatrix} v_m \\ F_m \end{pmatrix}.$$

Piezoelectrically active layer

Consider now a layer of piezoelectric material. An electric field (E) is applied across the layer. The layer could be interpreted as a parallel plate capacitor having a capacitance (C_0). In a piezoelectrically active layer the electro-acoustic coupling needs to be included. The force in this case is also dependent on the applied electric field as:

$$F = A(c \cdot S - eE) = ikcA(-a \cdot e^{-ikz} + b \cdot e^{ikz})e^{i\omega t} + I \frac{e/\epsilon^s}{i\omega}. \quad 20$$

I is the current as:

$$I = i\omega C_0 V - \frac{e}{\epsilon^s} C_0 (v_{pL} - v_{pR}),$$

where v_{pL} and v_{pR} is the acoustic displacement velocities at each border of the piezoelectric layer respectively and V is the applied voltage.

¹⁹ A is the area, X is the stress, S is the strain and c is the stiffness constant.

²⁰ e is the piezoelectric constant. ϵ is the dielectric permittivity.

For a piezoelectric layer the equation corresponding to eq. 3 would be:

$$\begin{pmatrix} v_{pL} \\ F_{pL} \\ I \end{pmatrix} = T_p \begin{pmatrix} v_{pR} \\ F_{pR} \\ V \end{pmatrix} \quad (4)$$

where T_p is a 3-by-3 transformation matrix.

The complete resonator structure

Consider now a piezoelectrically active layer with n number of layers on the left side and m number of layers on the right side (see fig below).

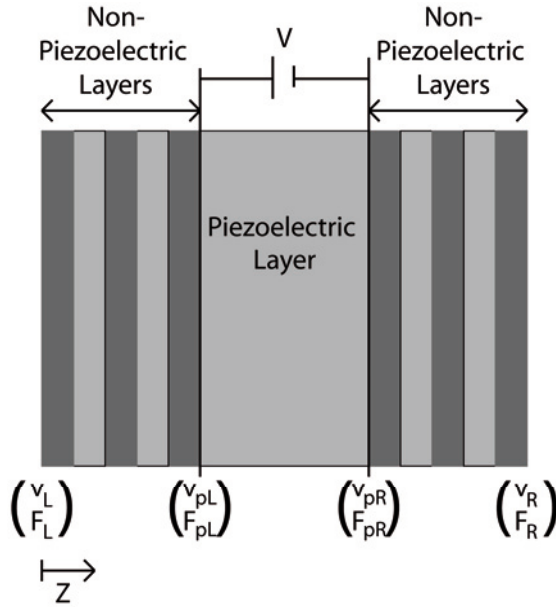


Figure 32. Schematic drawing of a complete resonator structure.

Left hand side:

$$\begin{pmatrix} v_L \\ F_L \end{pmatrix} = T_0 T_1 \cdots T_n \begin{pmatrix} v_{pL} \\ F_{pL} \end{pmatrix} = \hat{T}_L \begin{pmatrix} v_{pL} \\ F_{pL} \end{pmatrix}$$

Right hand side:

$$\begin{pmatrix} v_{pR} \\ F_{pR} \end{pmatrix} = T_R \begin{pmatrix} v_R \\ F_R \end{pmatrix}$$

Piezoelectric layer: as eq. 4.

Accordingly one can write:

$$\begin{pmatrix} v_{pL} \\ F_{pL} \\ I \end{pmatrix} = T_p \begin{pmatrix} v_{pR} \\ F_{pR} \\ V \end{pmatrix} = T_p \begin{pmatrix} T_R & 0 \\ & 0 \\ 0 & 0 & 1 \end{pmatrix} \begin{pmatrix} v_R \\ F_R \\ V \end{pmatrix} = \begin{pmatrix} inv(T_L) & 0 \\ & 0 \\ 0 & 0 & 1 \end{pmatrix} \begin{pmatrix} v_L \\ F_L \\ V \end{pmatrix}$$

And then the complete system could be described as:

$$\begin{pmatrix} v_L \\ F_L \\ I \end{pmatrix} = inv \begin{pmatrix} inv(T_L) & 0 \\ & 0 \\ 0 & 0 & 1 \end{pmatrix} T_p \begin{pmatrix} T_R & 0 \\ & 0 \\ 0 & 0 & 1 \end{pmatrix} \begin{pmatrix} v_R \\ F_R \\ V \end{pmatrix} = T^{total} \begin{pmatrix} v_R \\ F_R \\ V \end{pmatrix} \quad (5)$$

Assumptions used

Inhere the two outermost surfaces of the structure are always assumed to be free surfaces with zero input impedances. That is, the force (stress) is zero. This means that in the case of surrounding bulk liquid this has been modeled as a layer with one free surface in contact with vacuum. The thickness of the bulk liquid layer has always been large enough to ensure complete attenuation of the acoustic wave through the layer, so that the layer is thereby stated to be semi-infinitely thick in correspondence with the bulk liquid. The applied voltage is set to 1V. This gives that I , v_L and v_R are the only unknowns left in eq. 5.

From eq. 5 it can then be derived that:

$$v_R = -\frac{T_{2,3}^{total}}{T_{2,1}^{total}} V$$

$$v_L = T_{1,1}^{total} v_R + T_{1,3}^{total} V$$

$$I = T_{3,1}^{total} v_R + T_{3,3}^{total} V$$

$T_{i,j}^{total}$ is the element in row i column j of the matrix T^{total} .

From the above the impedance response (V/I) can be calculated as well as the solution inside each layer can be reconstructed (from eq. 1).

Acta Universitatis Upsaliensis

*Digital Comprehensive Summaries of Uppsala Dissertations
from the Faculty of Science and Technology 609*

Editor: The Dean of the Faculty of Science and Technology

A doctoral dissertation from the Faculty of Science and Technology, Uppsala University, is usually a summary of a number of papers. A few copies of the complete dissertation are kept at major Swedish research libraries, while the summary alone is distributed internationally through the series Digital Comprehensive Summaries of Uppsala Dissertations from the Faculty of Science and Technology. (Prior to January, 2005, the series was published under the title "Comprehensive Summaries of Uppsala Dissertations from the Faculty of Science and Technology".)



ACTA
UNIVERSITATIS
UPSALIENSIS
UPPSALA
2009

Distribution: publications.uu.se
urn:nbn:se:uu:diva-89424